

UNIVERSITY OF TARTU  
Faculty of Science and Technology  
Institute of Technology

Imane Muhammad Higazy

# **Investigation of Excitatory Ion Channels In Parkinsonian Sensory Neurons**

Master's Thesis (30 ECTS)

Curriculum Bioengineering

Supervisor(s):

Associate Professor, PhD Miriam A. Hickey, PhD Maili Jakobson

Tartu 2023

## **Investigation of Excitatory Ion Channels In Parkinsonian Sensory Neurons**

### **Abstract:**

**Background:** Parkinson's disease (PD) is associated with tremor, slowness of movement and stiffness, the latter two of which are caused by the loss of dopaminergic neurons of the substantia nigra pars compacta. Interestingly, although olfactory impairment is now well recognised in PD, skin symptoms differentiate individuals who go on to develop PD even better than olfactory impairment. However, little is known of the cause of this skin pathology, which includes proteinaceous aggregates and loss of peripheral neurites. Recently, several excitatory ion channels were found to be upregulated in PD patient skin. Here, we have examined the effect of overexpression of these channels in a sensory neuronal cell model of PD.

**Methods:** The 50B11 cell line, which is an immortalised DRG rat sensory neuronal cell line (kind gift from Dr Höke, Johns Hopkins University), was used. Familial PD was modelled by transfection with eGFP-alpha synuclein. Sporadic PD was modelled by treating with rotenone, a well-validated risk factor for PD and inhibitor of complex I. In our first series of experiments, cells overexpressing eGFP-alpha-synuclein or GFP (control plasmid) were treated with rotenone or DMSO and were then fixed for imaging and cytotoxicity analysis. In our second series, cells were co-transfected with alpha synuclein and HCN1 and then treated with rotenone or vehicle, then fixed for imaging and analysis of cytotoxicity. In our final series, cells were transfected with HCN1 or control plasmid, treated with rotenone or vehicle and then imaged live for mitochondrial membrane potential (MMP) and cell morphology.

**Results:** In our first series of experiments, the density of alpha synuclein-overexpressing cells was increased following rotenone exposure. However, in our second series, co-transfection of HCN1 with alpha synuclein resulted in lowered density of cells treated with rotenone. In our final series of experiments, rotenone caused a small reduction in MMP. HCN1 overexpression alone reduced MMP to a much greater degree. HCN1 overexpression exacerbated the effect of rotenone on MMP. This combination of HCN1 overexpression with rotenone changed the morphology of sensory neurons to a smaller, more rounded shape.

**Conclusions:** HCN1 is an important regulator of activity in sensory neurons and its overactivity is involved in several types of neuropathic pain. PD patients show loss of peripheral neurons and recently, HCN1 was found to be overexpressed in skin samples of PD patients. Although the normal function of alpha synuclein is unclear, it may induce proliferation and also may increase expression of anti-oxidant genes, and here, we found that alpha synuclein protected against rotenone toxicity. However, co-expression of HCN1 prevented this effect and resulted in increased cell death. In separate experiments, the combination of overexpression of HCN1 and rotenone resulted in exacerbated loss of mitochondrial membrane potential, and a change in cell shape indicative of toxicity. Thus, HCN1 overexpression may precipitate toxicity in parkinsonian sensory neurons and contribute to peripheral neuropathy in PD.

**Keywords:** Sensory neuropathy, HCN1, alpha synuclein, rotenone, dorsal root ganglion cells, familial Parkinson's disease, sporadic Parkinson's disease

**CERCS:** B640 Neurology, neuropsychology, neurophysiology

## **Eksitatorsete ionkanalite uurimine parkinsonismi mudeldavates sensoorsetes neuronites**

### **Kokkuvõte:**

**Taust:** Parkinsoni tõbe (PD) seostatakse värina, liigutuste aegluse ja jäikusega, millest viimased kaks on põhjustatud substantia nigra pars compacta dopaminergiliste neuronite hävinemisest. Huvitav on see, et kuigi nüüdseks on ka haistmismeele kahjustuse olemasolu PD puhul hästi äratuntav, eristuvad isikutel, kellel tekib PD, mitmed sümptomid nahas veelgi paremini kui kahjustused haistmises. Siiski on patoloogia põhjustest, mille hulka kuuluvad valgulised agregaadid ja perifeersete neuriitide kadu nahas väga vähe teada. Hiljuti leiti, et mitmed ergastavad ionkanalid on PD patsiendi nahas ülesreguleeritud. Käesolevas töös oleme uurinud nende kanalite üleekspressiooni mõju PD sensoorses neuropaatses rakumudelil.

**Meetodid:** Kasutati 50B11 rakuliini, mis on immortaliseeritud roti dorsaaljuure ganglionitest (DRG) pärinev sensoorne neuropaatsed rakuliin (kingitus dr. Höke'ilt, Johns Hopkinsi ülikool). Perekondlikku PD modelleeriti transfekteerides rake eGFP-alfa sünnukleiiniga. Sporaadilise PD modelleerimiseks töödeldi rakke rotenooniga, mis on hästi valideeritud PD riskifaktor ja mitokondriaalse hingamisahela kompleks I inhibiitor. Meie esimeses katseserias töödeldi eGFP-alfa-sünnukleini või GFP (kontrollplasmidi) üleekspresserivaid rake rotenooni või DMSO-ga, misjärel need fikseeriti pildistamiseks ja tsütotoksilisuse analüüsiks. Teises katseserias transfekteeriti rakke koos alfa-sünnukleini ja HCN1-ga ning töödeldi seejärel rotenooni või selle kandjalahusega ning seejärel rakud fikseeriti pildistamiseks ja tsütotoksilisuse analüüsimiseks. Meie viimases seerias transfekteeriti rakke HCN1 või kontrollplasmidiga, töödeldi rotenooni või selle kandjalahusega ja seejärel pildistati rakke mitokondriaalse membraanipotentsiaali (MMP) ja raku morfoloogia analüüsi jaoks.

**Tulemused:** Meie esimeses katseserias suurenes pärast rotenooniga kokkupuudet alfa-sünnukleini üleekspresserivate rakkude tihedus plaadil. Samas meie teises seerias vähendas HCN1 kotransfektsioon alfa-sünnukleiiniga rotenooniga töödeldud rakkude tihedust plaadil. Meie viimases katseserias põhjustas rotenoon MMP vähest alanemist rakkudes. Ainult HCN1 üleekspressioon vähendas MMP-d palju suuremal määral. HCN1 üleekspressioon võimendas rotenooni mõju MMP-le. See HCN1 üleekspressiooni kombinatsioon rotenooniga muutis sensoorsete neuronite morfoloogiat ka väiksemaks ja ümaramaks.

**Järeldused:** HCN1 on sensoorsete neuronite aktiivsuse oluline regulaator ja selle üleaktiivsus on seotud mitut tüüpi neuropaatilise valuga. PD patsientidel esineb perifeersete neuronite kadu ja hiljuti leiti, et PD patsientide nahaproovides on HCN1 üleekspresseritud. Kuigi alfa-sünnukleini normaalne funktsioon on ebaselge, võib see indutseerida proliferatsiooni ja suurendada ka antioksidantsete geenide ekspressiooni ning käesolevas töös leidsime, et alfa-sünnukleiin kaitseb rotenooni toksilisuse eest. Kuid HCN1 koekspressioon takistas seda efekti ja suurendas rakusurma. Eraldi katsetes põhjustas HCN1 üleekspressiooni ja rotenooni kombinatsioon mitokondriaalse membraanipotentsiaali halvenemist ja raku kuju muutust, mis viitab toksilisusele. Seega võib HCN1 üleekspressioon esile kutsuda parkinsonismi mudeldavates sensoorsetes neuronites toksilisuse ja aidata kaasa perifeerse neuropaatia tekkele PD korral.

**Märksõnad:** sensoorne neuropaatia; HCN1, alfa-sünnukleiin, rotenoon; dorsaaljuure ganglion; perekondlik Parkinsoni tõbi; sporaadiline Parkinsoni tõbi; 50B11.

**CERCS:** B640, neuroloogia, neuropsühhologia, neurofüsioloogia

## TABLE OF CONTENTS

TERMS, ABBREVIATIONS AND NOTATIONS .....	6
INTRODUCTION .....	8
1 LITERATURE REVIEW .....	9
1.1 Parkinson's disease (PD) Overview.....	9
1.2 PD Symptoms .....	9
1.3 PD Pathogenesis .....	10
1.4 Aetiology of PD (Risk Factors) .....	12
1.4.1. Environmental Risk Factors.....	12
1.4.2. Genetic Risk Factors .....	14
1.5 Peripheral Neuropathy (PN) and PD.....	16
1.5.1. Peripheral Neuropathy Pathological Overview.....	16
1.5.2. Epidemiology of Peripheral Neuropathy in PD .....	16
1.5.3. Pathophysiology of Peripheral Neuropathy in PD .....	17
1.5.4. Symptoms and Manifestation of Peripheral Neuropathy in PD.....	17
1.5.5. Excitatory Ion Channel Overexpression in PD Patient Skin.....	18
2 THE AIMS OF THE THESIS .....	20
3 EXPERIMENTAL PART .....	21
3.1 MATERIALS AND METHODS.....	21
3.1.1. Cell line .....	21
3.1.2. Plasmids .....	21
3.1.3. Cell seeding and Transfection.....	22
3.1.4. Treatment with Rotenone.....	22
3.1.5. Cell Fixing and Hoechst Staining .....	22
3.1.6. Microscopic Imaging of live cells.....	23
3.1.7. Analysis of Cytotoxicity in Fixed cells .....	26

3.1.8. Statistical Analysis .....	27
3.2 RESULTS .....	28
3.2.1 Effect of Overexpression of $\alpha$ -Synuclein on Parkinsonian 50B11 cells .....	28
3.2.2 Effect of Overexpression of HCN1 on Parkinsonian 50B11 cells .....	32
3.2.3 Effect of Overexpression of HCN1 on MMP .....	33
3.2.4 Effect of Overexpression of SCN2B on 50B11 cells .....	43
3.3 DISCUSSION .....	44
3.3.1. Effect of Overexpression of $\alpha$ -Synuclein and HCN1 on Cytotoxicity in Parkinsonian 50B11 cells .....	44
3.3.2. Effect of HCN1 on Mitochondria in Parkinsonian 50B11 cells .....	44
SUMMARY .....	46
REFERENCES .....	47
NON-EXCLUSIVE LICENCE TO REPRODUCE THESIS AND MAKE THESIS PUBLIC .....	58

## **TERMS, ABBREVIATIONS AND NOTATIONS**

<b>PD</b>	Parkinson's Disease
<b>NMS</b>	Non Motor Symptoms
<b>SNpc</b>	Substantia Nigra Pars Compacta
<b><math>\alpha</math>-Syn</b>	$\alpha$ -synuclein
<b>LB</b>	Lewy bodies
<b>MPTP</b>	1-methyl-4-phenyl-1,2,3,6-tetrahydropyridine
<b>SNCA</b>	Synuclein Alpha gene
<b>GWAS</b>	Genome wide association studies
<b>sPD</b>	sporadic
<b>LN<sub>s</sub></b>	Lewy neurites
<b>UPS</b>	Ubiquitin-Proteasome System
<b>LAS</b>	Lysosomal Autophagy System
<b>PN</b>	Peripheral neuropathy
<b>PNS</b>	Peripheral Nervous System
<b>SFN</b>	Small-Fiber Neuropathy
<b>LFN</b>	Large-Fiber Neuropathy
<b>L-DOPA</b>	Levodopa
<b>CIDP</b>	Chronic Inflammatory Demyelinating Polyneuropathy
<b>ENFs</b>	Epidermal Nerve Fibers
<b>MCs</b>	Meissner Corpuscles
<b>K<sub>v</sub></b>	Voltage-dependent Potassium

<b>HCN1</b>	Hyberpolarization activated cyclic nucleotide-gated channels
<b>CNS</b>	Central Nervous System
<b>PNS</b>	peripheral nervous system
<b>DRG</b>	dorsal root ganglion
<b>MMP</b>	Mitochondrial Membrane Potential
<b>TMRM</b>	Tetramethylrhodamine methyl ester
<b>DMSO</b>	Dimethyl sulphoxide
<b>PFA</b>	Paraformaldehyde
<b>PBS</b>	Phosphate buffered saline
<b>LTX</b>	Lipofectamine Reagent X
<b>cAMP</b>	Cyclic Adenosine Monophosphate

## INTRODUCTION

Parkinson's disease (PD) is the second most common common movement disorder, affecting 1–2% of the world's population over age of 65 (Alves et al., 2008). PD patients manifest a significant disability and decreased quality of life; where motor impairment represents a considerable burden in daily activity management (Hammarlund et al., 2018). A number of early non-motor symptoms, that are usually under-recognized and/or under-treated, have been identified and found to greatly impact PD patients' life quality, preceding the onset of motor-symptoms by several years (prodromal phase) (Wolters, 2009). Reported risk factors for developing PD include age, genetic and environmental factors (Kiebertz and Wunderle, 2013). However; etiology of the disease in most patients is still unclear (Balestrino and Schapira, 2020), and is thought to result from interaction between several risk factors.

An increased prevalence of peripheral neuropathy (PN) has been identified (Mancini et al., 2014), in up to 55% of PD patients' population (Comi et al., 2014). However; to date, no clear consensus on the underlying pathophysiology of PN in PD has been described (Kass-Iliyaa et al., 2015). Pathological findings concluded from skin biopsies in some PD patients, indicated an increased  $\alpha$ -synuclein deposition in cutaneous sympathetic adrenergic and sympathetic cholinergic fibers (Giannoccaro et al., 2015). Phosphorylated  $\alpha$ -synuclein has also been detected in the peripheral nervous system of PD patients, notably in the autonomic nerves of the colon, cardiac plexus, and cutaneous C-fibers (Donadio et al., 2014). Such findings led to perceiving skin tissue as a potential biomarker in PD (Doppler et al., 2014).

This thesis project is part of Dr. Pille Taba (Estonian Research Council "Team grant" project PRG957), Institute of Biomedicine and Translational Medicine in a joint project with the Tartu University Hospital to further investigate the peripheral nervous system involvement in PD. We set to find out whether peripheral neurons are more vulnerable to overexpression of excitatory ion channel subunits in PD model sensory neurons and whether their overexpression leads to mitochondrial dysfunction. Previous work in the Tartu University Hospital had shown upregulation of some excitatory ion channels in the skin of PD patients (Planken et al., 2017). In this thesis we are concerned with investigating the overexpression of HCN1 excitatory ion channel on parkinsonian 50B11 cells, in context of both genetic and environmental PD risk factors.

# **1 LITERATURE REVIEW**

## **1.1 Parkinson's disease (PD) Overview**

Parkinson's disease (PD) is the second-most common neurodegenerative disorder, affecting 1–2% of the world's population over the age of 65. Based on a global survey of neurological diseases in 2016, PD is considered one of the fastest growing neurological disorders worldwide. In terms of numbers, PD affects approximately 6.1 million people, with an expected doubling of incidence by year 2030 (Dorsey et al., 2007). Both the incidence and prevalence of PD have grown rapidly over the past two decades for not fully understood reasons (Dorsey et al., 2018), such that some have characterized it as a pandemic. PD is believed to result from an interaction of several predisposing factors including aging, environmental and genetic risk factors. To conclude, PD conveys a mounting socioeconomic burden, as it affects patients and society enormously. For patients, the disease duration can span decades, typically through a slow progression with accumulating disability over years. Caregivers and medical care systems are also profoundly affected (Bloem et al., 2021).

## **1.2 PD Symptoms**

Clinically, PD is known as “progressive movement disorder”, where motor impairment represents a considerable burden due to the significant disability in managing daily activities (Sjödahl Hammarlund et al., 2018). Typically, the onset of motor symptoms is asymmetric, then becomes bilateral over time (DeMaagd & Philip, 2015). Furthermore, a number of early non-motor symptoms have been identified and found to greatly impact the patient's life quality. Unfortunately, these are usually under-recognized and/or under-treated (Noyce et al., 2016) (see Figure 1).

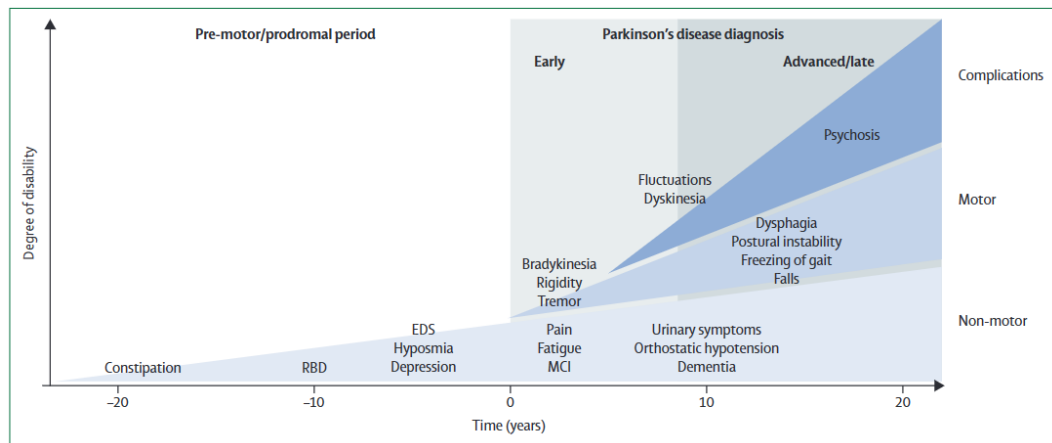


**Figure (1). Clinical symptoms and time course of Parkinson's disease progression**  
(Kalia & Lang, 2015)

PD diagnosis is based upon motor symptoms (time 0 years). These can be preceded, by 20 years or more, by a pre-motor/prodromal phase characterized by certain non-motor symptoms. More non-motor features develop with disease progression, resulting in clinically significant disability. Axial motor symptoms, as postural instability with frequent falls and freezing of gait, tend to occur in advanced PD. Long-term complications of dopaminergic therapy, such as fluctuations, dyskinesia, and psychosis, also contribute to disability. EDS=excessive daytime sleepiness, MCI=mild cognitive impairment, RBD=REM sleep behavior disorder.

Study of non-motor symptoms (NMS) has provided insights into the pathogenic processes underlying PD and has introduced PD as a propagating, multi-system disorder that affects both peripheral and central nervous systems, with motor functions manifesting at a relatively late stage (Kalia & Lang, 2015). Consequently, PD diagnosis is principally clinical at its late stages, with currently available therapeutics offering good control of motor symptoms, without affecting disease evolution or underlying cause (Balestrino & Schapira, 2020).

### 1.3 PD Pathogenesis

Neuropathological diagnostic markers of idiopathic PD have long been defined by dopaminergic neuronal loss in substantia nigra pars compacta (SNpc). This is coupled with subsequent loss of striatal dopamine content and deposition of misfolded  $\alpha$ -synuclein ( $\alpha$ -Syn) within intracytoplasmic inclusions called Lewy bodies (LB). Such altered forms of  $\alpha$ -synuclein spread from one affected neuron to the adjacent unaffected one in a prion-like manner. As misfolded  $\alpha$ -Syn acts as a seed and causes misfolding of monomeric  $\alpha$ -Syn (Z. Wang et al., 2021), this perpetuates the cycle of  $\alpha$ -synuclein misfolding and, hence, PD propagation (Kim et al., 2019). LB also include ubiquitin and small amounts of several other proteins (Mahul-Mellier et al., 2020).

The neuropathological picture of PD involves several additional regions, including locus coeruleus, brain stem reticular formation, raphe nucleus, dorsal motor nucleus of the vagus, nucleus basalis of Meynert, amygdala, and hippocampus (Jellinger, 2012). Presence of LB in peripheral tissues has widened our understanding of PD pathophysiology. LB pathology and  $\alpha$ -synuclein deposition are proposed to originate in the olfactory bulb and lower brain stem, from where they spread to midbrain, then cortical regions. This caudorostral spread of LB and  $\alpha$ -synuclein pathology in PD was first proposed by Braak and colleagues in 2003 (Braak et al., 2003) and has been modified over the intervening years (see Figure 2).

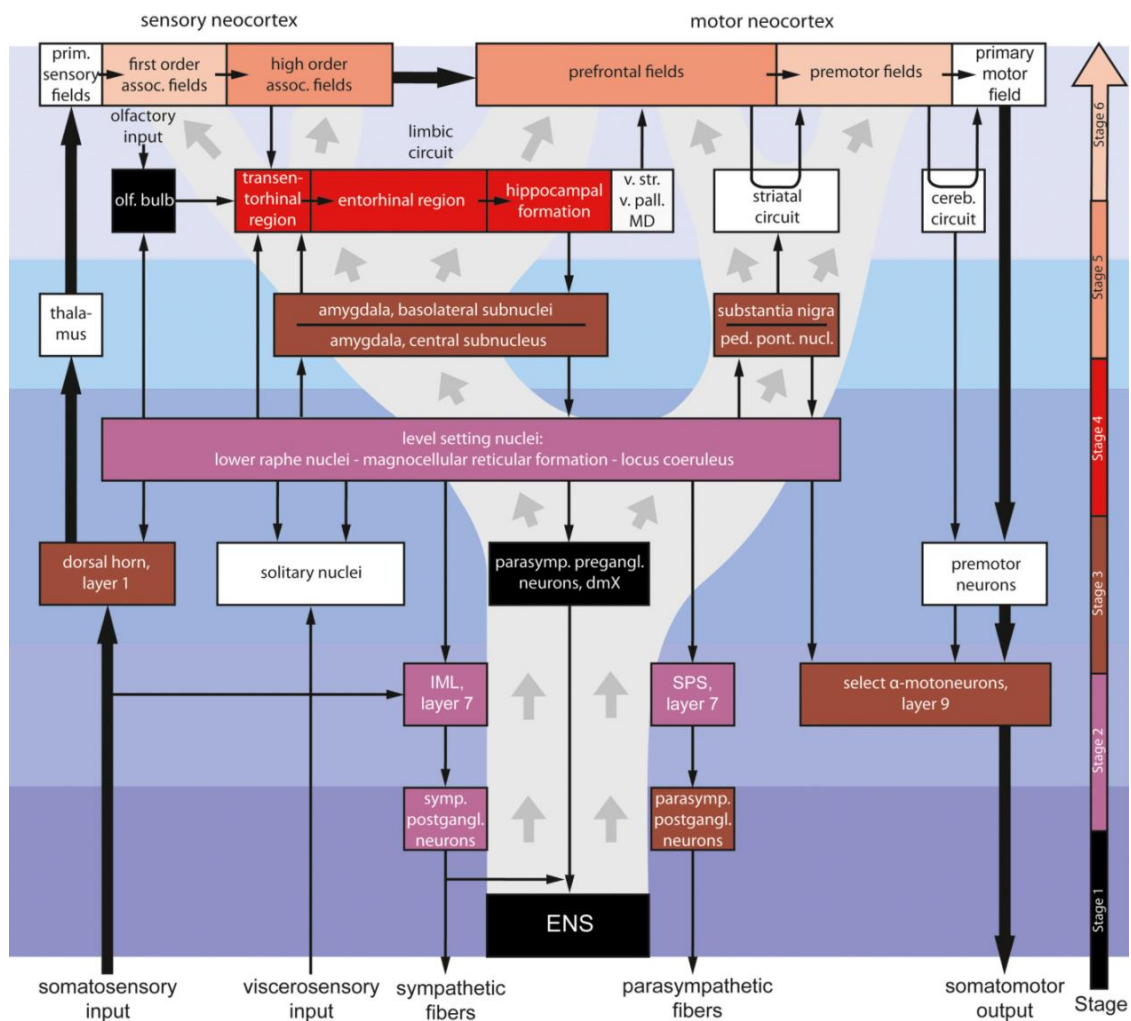


**Figure (2). Schematic Representation of the Braak's Hypothesis of PD**

(Del Tredici & Braak, 2016)

The orderly progression of aggregates of alpha synuclein proposed by Braak and colleagues. Stage I: Black. Stage II: Violet. Stage III: Brown. Stage IV: Bright red. Stage V: Peach/Orange. Stage VI: Light orange. Note that the substantia nigra pars compacta remains unaffected until Stage III.

## 1.4 Aetiology of PD (Risk Factors)

The aetiology of PD in most patients remains unclear; however, predisposing risk factors for developing PD include aging, genetic susceptibility, and environmental hazards (see Figure 3). Individually, each of these risk factors can only explain a small fraction of PD; however, their effects increase when they simultaneously interact (Van Den Eeden, 2003).

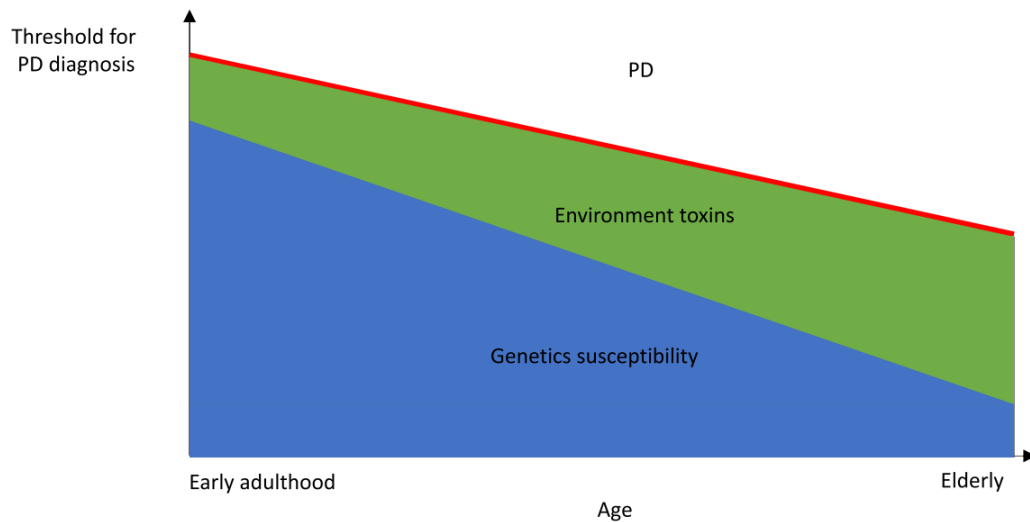


**Figure (3). Interaction between aging, genetic and environmental risk factors in PD pathogenesis**  
(Pang et al., 2019)

Red line: threshold of DA neuronal stress over which PD manifests. As age increases, impairment in cellular pathways increases susceptibility of DA neurons degeneration, thus lowering the threshold for developing PD. At a younger age, genetic predisposition plays major role in causing PD, while cumulative exposure to environmental toxins contributes significantly to PD development in old age.

### 1.4.1. Environmental Risk Factors

The aetiology of PD remained elusive to clinicians and researchers until two major discoveries, the first of which was MPTP-induced parkinsonism, introduced by Langston and colleagues in 1983 (Langston et al., 1983). MPTP (1-methyl-4-phenyl-1,2,3,6-tetrahydropyridine) is a contaminant found in synthetic heroin. The second was the discovery of SNCA (Synuclein Alpha gene) and the first genetic cause of PD in 1997 (Polymeropoulos et al., 1997). Discovery of PD induced by MPTP led to the hypothesis that environmental toxins can cause PD. Meta-analyses involving studies of environmental risk factors reported six main environmental factors as highly associated with PD incidence (Bellou et al., 2016) (see Table 1).

**Table (1). Environmental risk factors of PD and their biologic correlates (Pang et al., 2019)**

Risk Factors	Biologic Correlates
Pesticides	• Mitochondrial toxins, oxidative stress
Dairy	• Urate-lowering effects of dairy products
Traumatic brain injury	• Breakdown of blood-brain barrier, brain inflammation, impaired mitochondrial function, increase in glutamate release, $\alpha$ -synuclein accumulation
Anxiety or depression	• May be prodromal symptom rather than risk factor due to loss of serotonergic neuronal cells in dorsal raphe nucleus in early PD
Beta-blockers	• Aggravate the loss of norepinephrine neurons in locus coeruleus and deficits in norepinephrine in PD

#### 1.4.1.1. Rotenone exposure as a model of environmentally induced PD

Rotenone ([2R-(2 $\alpha$ ,6 $\alpha$ ,12 $\alpha$ )]-1,2,12,12a-tetrahydro-8,9-dimethoxy-2-(1-methylethenyl) [1] benzopyran [3,4-b] furo [2,3-h][1] benzopyran-6(6aH)-one) is an organic pesticide, naturally derived from roots, seeds and stems of several tropical plants as *Pachyrhizuserosus*(jicama vine), *Derris*, *Tephrosia*, *Lonchocarpus* and *Mundulea* species (Innos & Hickey, 2021). The Agricultural Health Study (AHS) found that PD was positively associated with exposure to two groups of pesticides, which were experimentally identified as impaired mitochondrial function (rotenone) and increased oxidative stress (paraquat) (Hatcher et al., 2008). More precisely speaking, it has been reported that farmers consistently exposed to rotenone were 2.5 times more likely to develop PD compared to non-rotenone users (Tanner et al., 2011).

Rotenone was first used by Heikkila *et al.* in 1985 to model PD by stereotaxic administration into rat brain (Heikkila et al., 1985). Rotenone has ever since been used in modeling PD both *in-vivo* and *in-vitro*. In our study, we have used rotenone to model environmental risk factors. The lipophilic nature of rotenone permits its free transport across cellular membranes [for review see (Innos & Hickey, 2021)], independent of any transporter. This facilitates its action as a mitochondrial toxin (see Figure 4), where it inhibits mitochondrial complex I of the respiratory chain, resulting in increased levels of reactive oxygen species and reduced ATP production (Friedrich et al., 1994). Importantly, increased oxidative stress causes  $\alpha$ -synuclein aggregation.

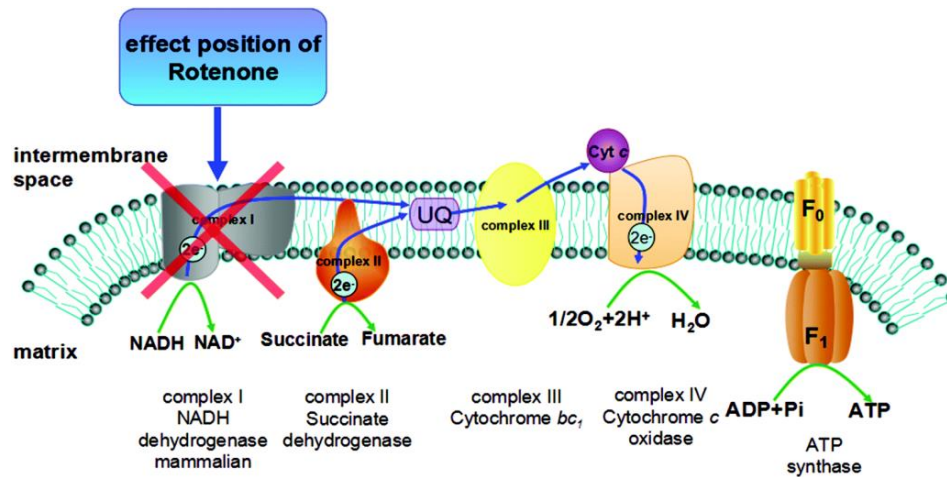


**Figure (4). Mechanism of Rotenone as a mitochondrial toxin** (Xu et al., 2016)

Rotenone acts on the coupling site of NADH- coenzyme Q oxidoreductase, inhibiting oxidative phosphorylation

### 1.4.2. Genetic Risk Factors

GWAS has identified mutations in more than 20 genes that contribute to increased PD susceptibility (Nalls et al., 2019), with genetic risk generally divided into two categories; rare coding variants with high effect size and more common variants with small effects (see Table 2). The former are typically associated with monogenic or familial PD, while the latter are usually identified in sporadic PD (Nalls et al., 2019). Historically, PD had been long considered as a purely sporadic disorder, with almost 85-90% of cases identified as sporadic (sPD) with no clear defined cause. The remaining 5-15% of patients has monogenic/familial PD (DeL Rey et al., 2018).

Although studying genetics of PD has provided interesting insight on its pathogenesis (Balestrino & Schapira, 2020), it became apparent that different forms of PD have varying degrees of genetic and environmental components interacting at different levels (Pang et al., 2019). Thus, here we have examined both genetic and environmental risk factors. We have chosen SCNA as our genetic risk factor. SNCA variants have been identified to contribute to both familial and sporadic forms of PD (Poewe et al., 2017).

**Table (2). List of most common genes associated with PD (Poewe et al., 2017)**

Locus symbol	New designation <sup>†</sup>	Gene locus	Gene	OMIM (phenotype MIM number; gene/locus MIM number)	Clinical clues
<b>Autosomal dominant Parkinson disease</b>					
PARK1 or PARK4	PARK-SNCA	4q22.1	SNCA	• 168601; 163890 (PARK1) • 605543; 163890 (PARK4)	Missense mutations (PARK1) cause classic Parkinson disease phenotype. Duplication or triplication of this gene (PARK4) causes early-onset Parkinson disease with prominent dementia
PARK8	PARK-LRRK2	12q12	LRRK2	607060; 609007	Classic Parkinson disease phenotype. Variations in LRRK2 include risk-conferring variants and disease-causing mutations
PARK17	PARK-VPS35	16q11.2	VPS35	614203; 601501	Classic Parkinson disease phenotype
<b>Early-onset Parkinson disease (autosomal recessive inheritance)</b>					
PARK2	PARK-Parkin	6q26	PARK2 encoding parkin	600116; 602544	Often presents with lower limb dystonia
PARK6	PARK-PINK1	1p36.12	PINK1	605909; 608309	Psychiatric features are common
PARK7	PARK-DJ1	1p36.23	PARK7 encoding protein deglycase DJ1	606324; 602533	Early-onset Parkinson disease
PARK19B	PARK-DNAJC6	1p31.3	DNAJC6	615528; 608375	Onset of parkinsonism between the third and fifth decades of life
<b>Complex genetic forms (autosomal recessive inheritance)<sup>‡</sup></b>					
PARK9	PARK-ATP13A2	1p36.13	ATP13A2	606693; 610513	Early-onset parkinsonism with a complex phenotype (for example, dystonia, supranuclear gaze palsy, pyramidal signs and cognitive dysfunction); also known as Kufor–Rakeb syndrome
PARK14	PARK-PLA2G6	22q13.1	PLA2G6	256600; 603604	PLAN (or NBIA2) is characterized by a complex clinical phenotype, which does not include parkinsonism in the majority of cases
PARK15	PARK-FBXO7	22q12.3	FBXO7	260300; 605648	Early-onset parkinsonism with pyramidal signs and a variable complex phenotype (for example, supranuclear gaze palsy, early postural instability, chorea and dystonia)
PARK19A	PARK-DNAJC6	1p31.3	DNAJC6	615528; 608375	Juvenile-onset parkinsonism that is occasionally associated with mental retardation and seizures
PARK20	PARK-SYNJ1	21q22.11	SYNJ1	615530; 604297	Patients may have seizures, cognitive decline, abnormal eye movements and dystonia
PARK23	Not yet assigned	15q22.2	VPS13C	616840; 608879	Young-adult-onset parkinsonism associated with progressive cognitive impairment that leads to dementia and dysautonomia

<sup>†</sup>The locus symbols are in accordance with the Online Mendelian Inheritance in Man (OMIM) catalogue (<https://omim.org>)

#### 1.4.2.1. SCNA gene

As stated above, mutations in the SNCA gene were identified as the first genetic cause of PD (Polymeropoulos et al., 1997). Alpha-synuclein is a natively unstructured, presynaptic neuronal protein that is post-translationally modified. It is thought to adopt distinct conformations in dynamic equilibrium, based upon the cellular milieu. However, such homeostasis becomes altered in disease states (Winner et al., 2011). As stated above,  $\alpha$ -synuclein ( $\alpha$ -Syn) represents the major constituent of LBs and Lewy neurites (LNs), one of the pathological hallmarks of PD (Spillantini et al., 1997).

Patients carrying SNCA mutations usually present with a younger age at onset, with early and severe non-motor symptoms. Both point mutations and gene multiplications have been reported for the SNCA gene (Poewe et al., 2017). Several isoforms of  $\alpha$ -Syn have been implicated in PD pathogenesis; however,  $\alpha$ -Syn oligomers formed during  $\alpha$ -Syn aggregation are thought to be the most toxic (Alam et al., 2019). Interestingly,  $\alpha$ -Syn aggregates are observed in peripheral tissues of PD patients, e.g., skin, olfactory mucosa, salivary gland, gut

mucosa and gonadal tissue (Fayyad et al., 2019), and all of these tissues show dysfunction in PD.

Aggregates of  $\alpha$ -Syn exert a detrimental effect on surviving neurons in many ways, including inhibition of the ubiquitin-proteasome system (UPS), induction of endoplasmic reticulum stress, mitochondrial dysfunction and impaired synaptic function (Alam et al., 2019)

## **1.5 Peripheral Neuropathy (PN) and PD**

### **1.5.1. Peripheral Neuropathy Pathological Overview**

Peripheral neuropathy (PN) generally refers to any disorder of the peripheral nervous system (PNS) including single and multiple mononeuropathies (mononeuritis multiplex), symmetrical involvement of many nerves (polyneuropathy) or isolated involvement of sensory ganglia (ganglionopathies). PN can also manifest as postural instability, loss of peripheral sensation, weakness and/or pain, and it can be divided into small-(unmyelinated C fibers and thinly myelinated A $\delta$  fibers) and large-fiber (axonal) neuropathy. Further classification relies on phenomenological, neurophysiological, pathological, and aetiological aspects (Zis et al., 2017).

### **1.5.2. Epidemiology of Peripheral Neuropathy in PD**

An increasing number of studies have reported an elevated prevalence of PN in PD population, challenging the traditional view of PD as a disorder of the central nervous system. The prevalence of PN in PD varies depending upon the diagnostic methods employed. Similar to constipation, a very common feature of PD, PN is rarely considered serious by patients and is therefore likely underdiagnosed. However, specific analysis of neurite number in skin shows a high prevalence of PN in PD (Zis et al., 2017). For example, up to 55% of PD patients (Comi et al., 2014), compared to 8–9% in general population of similar age (Misra et al., 2008), show PN.

### **1.5.3. Pathophysiology of Peripheral Neuropathy in PD**

Pathological findings from skin biopsies in some PD patients indicate a reduction in small-fiber density compared to healthy controls [reviewed in (Comi et al., 2014; Zis et al., 2017)], as well as an increased deposition of  $\alpha$ -Syn in cutaneous sympathetic adrenergic and sympathetic cholinergic fibers (N. Wang et al., 2013). Moreover; phosphorylated  $\alpha$ -Syn has also been detected in the peripheral nervous system of PD patients, notably in autonomic nerves of the colon, cardiac plexus, and cutaneous C-fibers (Donadio et al., 2014). Furthermore; a correlation between neuritic  $\alpha$ -Syn inclusions and small-fibre neuropathy has been reported, suggesting a possible direct role of phosphorylated  $\alpha$ -Syn in peripheral nerve fiber damage (Vacchi et al., 2021). Such findings led to perceiving skin tissue as a potential biomarker in PD.

It has been suggested that PN in PD might be linked to Levodopa (L-DOPA) intake, due to a reported increased prevalence of PN in patients treated with L-DOPA (Romagnolo et al., 2019). However, other studies suggested PN as a possible intrinsic feature of PD (Lee & Baik, 2020). Furthermore, population-based studies indicated an increased prevalence of skin complaints and abnormalities in skin sensation of PD patients prior to their diagnosis, i.e., at the prodromal stage (Schrag et al., 2023). This highlights the probability that intrinsic pathogenetic features of PD may predispose to PN. Importantly, PN in PD can lead to an increase in the disability of patients, resulting in an additional motor dysfunction (Corrà et al., 2023), finally worsening of overall functional mobility.

### **1.5.4. Symptoms and Manifestation of Peripheral Neuropathy in PD**

PD patients manifest a number of skin symptoms including cutaneous neuropathy, seborrhoea, hyperhidrosis and impaired wound healing (Beitz, 2013). The majority of cases of PN in PD manifest as distal, symmetrical, axonal and predominantly sensory (Zis et al., 2017). A significant increase in tactile and thermal thresholds, as well as significant reduction in mechanical pain perception and loss of epidermal nerve fibers (ENFs) and Meissner corpuscles (MCs) (Nolano et al., 2008).

### **1.5.5. Excitatory Ion Channel Overexpression in PD Patient Skin**

In a study of PD patientskin, by Planken et al. (Planken et al., 2017), transcriptomics suggested large basal defects in cellular bioenergetics and mitochondrial dysfunction, impaired protein metabolism, dysbalanced skin homeostasis, deregulation of nuclear processes, as well as disturbances in many central signaling and immune pathways. They also found an increase in expression of several ion channels, including HCN1, and the accessory subunit SCN2b.

#### **1.5.5.1. HCN1 Excitatory Ion Channel**

HCN channels belong to the family of voltage-dependent potassium ( $K_v$ ) and cyclic nucleotide-gated (CNG) channels. The HCN family consists of four main isoforms (HCN1-4), whose biophysical properties and tissue distribution differ substantially within the nervous system and beyond. They are considered key players in controlling and facilitating neuron excitability, as they are uniquely dually activated by voltage hyperpolarization and intracellular cAMP (Biel et al., 2009). HCN channels are involved in a wide variety of neuronal processes including sensory signal transduction, dendritic integration, synaptic plasticity, pacemaking, network oscillations, motor learning, and others. Besides the central nervous system (CNS), HCN channels are widely expressed in the peripheral nervous system (PNS), where they are involved in perception, modulation, and transmission of sensory signals, including pain (Benzoni et al., 2021).

HCN channels are widely expressed and considered a major player in DRG excitability (Alles & Smith, 2021). Accumulating evidence supports the view that modifications in HCN channels physiological function contribute to pathogenic mechanism leading to certain neurological diseases in humans such as epilepsy, pain, and, as recently emerged, PD (DiFrancesco & DiFrancesco, 2015).

#### **1.5.5.2. SCN2B Ion Channel Regulatory Subunits**

Sodium channel gene mutations have been identified as one of the causes of PN, since voltage-gated sodium channel has a key role in regulating neuronal excitability (Alles & Smith, 2021). Sodium channels are mainly composed of a pore-forming  $\alpha$  subunit, associated with auxiliary  $\beta$  subunits. The  $\alpha$  subunit is expressed preferentially in the peripheral nervous system. Hence, they have been genetically and functionally identified as drivers of chronic

pain in humans; however, the contribution of  $\beta$  subunits to pain is still under investigation. The sodium channel  $\beta$  subunit is made up of four genes, SCN1B–SCN4B, and two splice variants,  $\beta$ 1A and  $\beta$ 1B (Catterall et al., 2020). Upregulation of the  $\beta$ 2 subunit has been shown to regulate both translocation and immobilization of sodium channels in the cell membrane and modify their kinetics, resulting in membrane hyperexcitability and ectopic activity, thereby contributing to neuropathic pain (Pertin et al., 2005). Furthermore; functional analysis showed that certain mutations in  $\beta$  subunits could enhance dorsal root ganglion (DRG) neuronal action potential firing; which is consistent with its contribution to pain in patients (Alsaloum et al., 2021).

## **2 THE AIMS OF THE THESIS**

To examine the effect of overexpression of HCN1 excitatory ion channel on mitochondrial membrane potential and cytotoxicity in parkinsonian sensory neurons.

To achieve this aim, I examined the effect of HCN1 overexpression

- 1) in the context of rotenone (an environmental risk factor for PD) and inhibitor of complex I of the electron transport chain
- 2) in the context of alpha synuclein overexpression (a genetic risk factor for PD)
- 3) in the context of both rotenone and alpha synuclein overexpression

### 3 EXPERIMENTAL PART

#### 3.1 MATERIALS AND METHODS

##### 3.1.1. Cell line

In our experiments, the 50B11 cell line was employed, which is an embryonic (E14.5) rat nociceptive dorsal root ganglia (DRG)- derived immortalized sensory neuronal cell line 50B11, that was gifted to us by Prof. Ahmet Höke of Johns Hopkins University, USA. 50B11 cells were cultured in Neurobasal™ medium (Catalog no. 21103049, Gibco™), supplemented with 10% fetal bovine serum (FBS), (Catalog no. A5256801, Gibco™), 2% B-27™ Supplement (Gibco™, ThermoFisher™ Scientific, USA), 20mM D-glucose, 0.2 M L-glutamine (GlutaMAX™ supplement, Catalog no. 35050087, Thermo Fisher™ scientific, USA). The 50B11 cells were incubated at 37°C, in atmospheric oxygen and humidity.

##### 3.1.2. Plasmids

Plasmid DNA was propagated by using DH5 $\alpha$  cells with respective antibiotics in LB broth for 12-16 h, in a shaking incubator at 37°C, 225 rpm and isolated with a Maxiprep kit (PureLink® HiPure Plasmid Filter Maxiprep Kit, Invitrogen, Life Technologies, USA), according to manufacturer's instructions, except that the DNA was dissolved in sterile water. Plasmid DNA concentration was measured using Thermo Scientific™ NanoDrop™ 2000/2000c spectrophotometer. The list of plasmids used is provided in table 3.

**Table (3). List of plasmids used in our experiments**

<b>Plasmids</b>	<b>Catalog name</b>	<b>Provider/Catalog #</b>
<b><math>\alpha</math>-Synuclein-WT-eGFP</b>	EGFP-alphasynuclein-WT	Addgene/ 40822
<b>GFP</b>	pAAV-hSyn-EGFP	Addgene/ 50465
<b>HCN1</b>	-	Kind gift from Prof. Noriyuki Nakashima, Kurume University, Japan
<b>Control plasmid</b>	pRL Renilla Luciferase	Kind gift from Prof A Kaasik, University of Tartu
<b>SCN2b</b>	HsCD00512658	Arizona Repository

### **3.1.3. Cell seeding and Transfection**

50B11 cells were seeded 24h before transfection (Day 0) into four-quadrant glass-bottomed cell culture dishes (CellVis, Mountain View, CA, USA, approximately 75000-100000 per quadrant). Cells were transfected in Opti-MEM™ Reduced serum medium (Gibco™, ThermoFisher™ Scientific, USA), using Lipofectamine™ LTX kit (Catalog no A12621, Invitrogen, ThermoFisher™ Scientific, USA), according to the manufacturer's instructions, with slight modifications. 500 and 750 ng DNA was used for double and triple co-transfection, respectively.

In brief, DNA was diluted in Opti-MEM™ medium, then Plus™ Reagent was added. DNA mixture was then incubated for 2-5min min at room temperature, before being added to LTX mix. The DNA-LTX mixture was incubated for 20 min, to allow DNA-LTX complexes to form. Normal culture medium was removed from each quadrant and replaced with a mixture of (250µl Opti-MEM™ + 50 µl DNA-LTX mixture). Cells were then incubated for 3.5-4h under atmospheric oxygen and humidity levels at 37°C. After 4h, the (Opti-MEM™ + DNA-LTX) the medium was replaced to fresh normal cell culture growth medium.

### **3.1.4. Treatment with Rotenone**

For rotenone treatment, cell culture medium containing 100nM rotenone in DMSO was applied to cells at 24h after transfection and were then incubated for 48 hours. DMSO served as a vehicle control. Cells were then imaged live or were fixed and stained. Both the rotenone concentration used and the incubation period have been determined and optimized in a previous study carried by our research group.

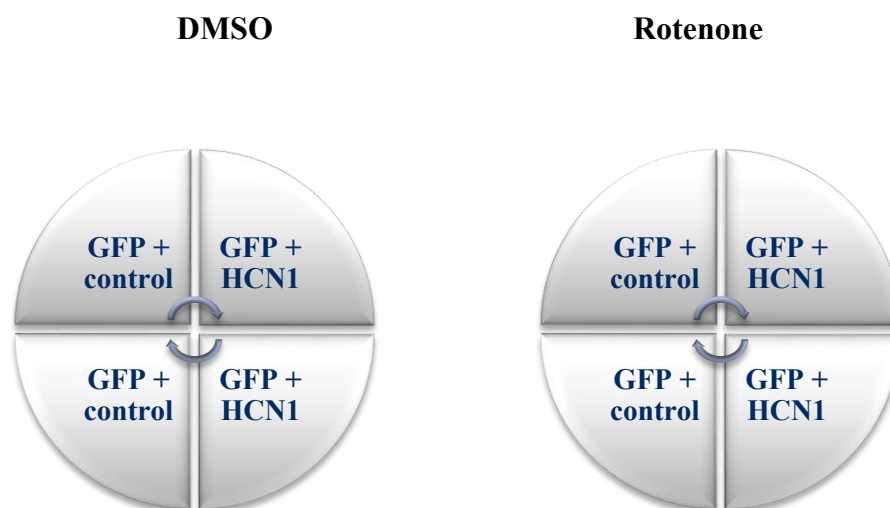
### **3.1.5. Cell Fixing and Hoechst Staining**

50B11 cells were fixed with 500ul per quadrant of 4% PFA in PBS containing 250µM sucrose for 10 mins, then washed and stained with Hoechst (1µg/ml) for 5mins, then washed and fluorescence mounting medium added. Plates were then stored at +4°C until imaging.

### 3.1.6. Microscopic Imaging of live cells

For measuring MMP, TMRM was employed. Tetramethylrhodamine methyl ester (TMRM, Invitrogen™, ThermoFisher™, USA) is a lipophilic cationic fluorescent probe that accumulates within polarized mitochondria. Thus, hyperpolarized mitochondria will accumulate more cationic dye, and vice versa. TMRM can be employed in either quenching or non-quenching mode. In our present study, the latter was used, which is appropriate for acute treatments (Perry et al., 2011). Cells were loaded with 10nM TMRM reagent in regular cell culture growth medium, and then incubated for 20 min at 37°C, at atmospheric levels of oxygen and humidity. For each quadrant, up to 10 images were taken.

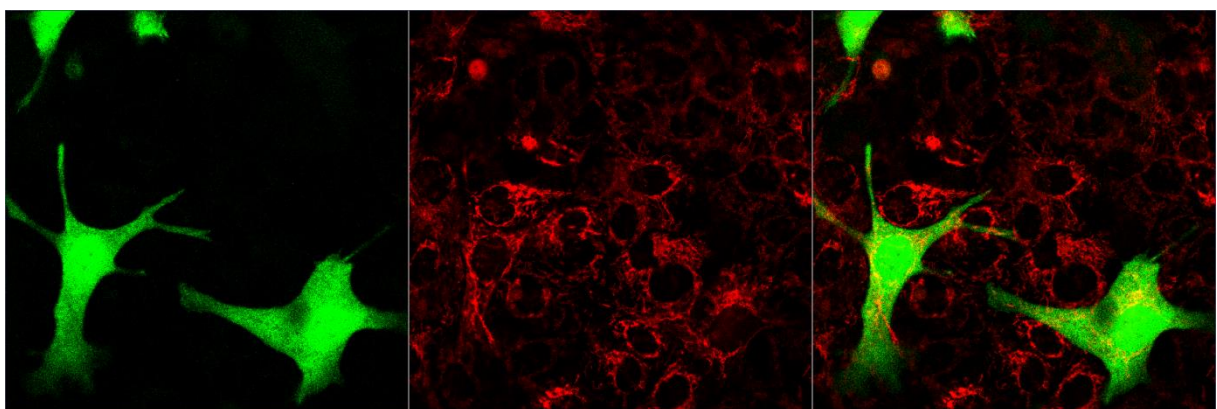
Cell culture dishes were placed in the confocal incubation chamber (maintained at 37°C). Images were taken using a Carl Zeiss Laser Scanning Microscope (LSM 780) using a 40x objective (numerical Aperture: 0.25, working distance: 7.45mm, ex 561 nm, em 566-669 nm). Images were processed using Zen software (2010) and analyzed using ImageJ (Fiji, v1.54d, National Institutes of Health (NIH) and the Laboratory for Optical and Computational Instrumentation (LOCI), University of Wisconsin). Each experiment contained at least two technical repeats and was itself considered one biological replicate. Data were generated from at least three biological replicates (see Figure 5).



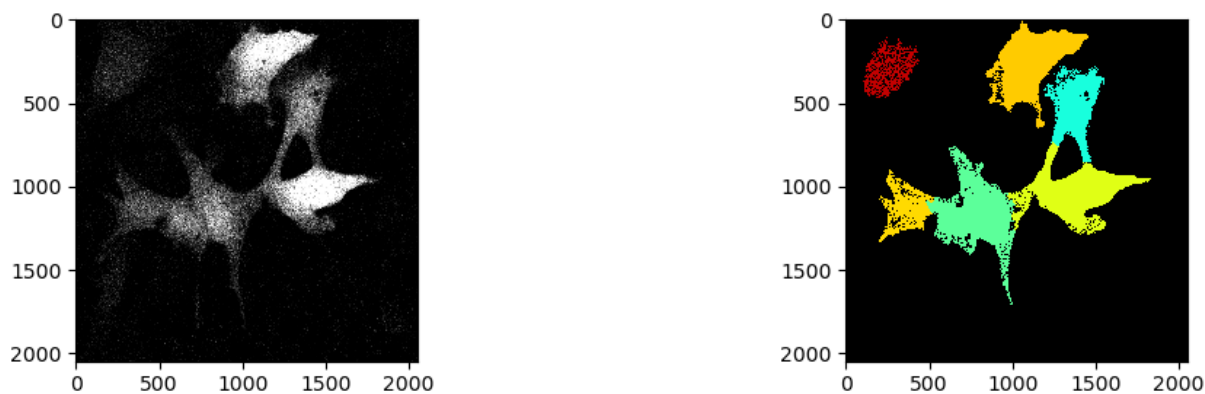
**Figure (5). General experimental design for TMRM analysis**

For analysis of TMRM images, the researcher was completely blinded to all treatments. Images were split into two channels, green and red (see Figure 6). Green showed transfected cells (HCN1 + GFP co-transfected or GFP-only transfected). Previous data from our lab has shown a high rate of co-transfection if 50B11 cells are transfected with several plasmids at once (personal communication Dr Maili Jakobson). Red showed TMRM fluorescence (figure (6)). Transfected cells and their corresponding mitochondria were outlined using the freehand tool in ImageJ (Fiji) software. Size of cell (from the green channel) and mean red fluorescence intensity and integrated density of red fluorescence was quantified, thus providing per-cell analyses. Mitochondria of untransfected cells (that did not show green fluorescence) were also outlined to provide additional controls. To ensure consistency in our analyses, a sample representing 25% of all images was analyzed to identify possible variations in cells that could affect outcome measures. Thus, a matrix was created to classify cells and prevent variability affecting outcomes (see Table 4).

For analysis of cell morphology, based upon green fluorescence, a CellProfiler algorithm was used. Briefly, channels were separated and transfected cells in the green channel were identified for morphological analysis using the solidity and form factor readouts (see Figure 7). Solidity as defined by Cell profiler software as “a differentiator of cells with protrusions or irregular shape versus generally round cells”. The higher the value of solidity, the more spherical the cell should be. “Form factor” is calculated as  $4*\pi*Area/Perimeter^2$ . A value of 1 denotes a perfectly circular object. CellProfiler is a freely available image analysis software: (Stirling et al., 2021)

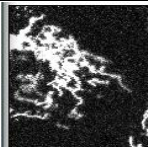
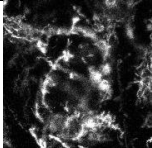
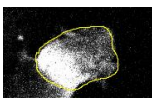
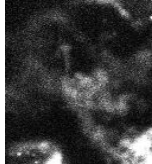


**Figure (6). Example green (left, GFP), red (middle, TMRM) and merged fluorescence.** Cells are transfected with HCN1 + GFP (previous data from our lab has shown a high rate of co-transfection in this cell line when they are transfected with several plasmids). Several cells are not transfected with GFP, and therefore not with HCN1. Thus, we have the ability to examine mitochondrial membrane potential in cells expressing HCN1 + GFP (or GFP only) and in cells that were not transfected.



**Figure (7).** Example of CellProfiler segmentation of GFP signal in transfected cells, for subsequent morphological analysis. Numbers on axes indicate pixels as CellProfiler converts all images to pixels.

**Table (4).** TMRM Image analysis Exclusion Matrix

	Cell description	Confocal Images	Reason for not Counting the cells
1	Corner-positioned		less than 75% of cell is shown
2	Overlapping Cell		complete overlapping
3	Cells appearing in transfected green channel with two colour intensities		difference in colour intensity is unjustified
4	Out of focus		cell borders are not completely defined

### 3.1.7. Analysis of Cytotoxicity in Fixed cells

Cells overexpressing GFP- $\alpha$ -synuclein (a genetic risk factor for sporadic PD) or cells expressing GFP were treated with rotenone or DMSO for 48hrs, and were then fixed with 4%PFA-sucrose, stained with Hoechst and imaged. Each experiment was carried in triplicate with at least two technical repeats within each experiment. This was performed to establish, for the first time, the  $\alpha$ -syn overexpression model in 50B11 cells.

Cells were imaged using an LSM780 confocal (N=8-30 images per quadrant; imaged using 10x objective; 1.66 $\mu\text{m}^2$  pixel size, 850 $\mu\text{m}^2$  image size; GFP ex 488nm em 498-598nm; Hoechst ex 405nm em 410-498nm). Images were analyzed using ImageJ (Fiji, v1.54d, National Institutes of Health (NIH) and the Laboratory for Optical and Computational Instrumentation (LOCI), University of Wisconsin) by a blinded observer. Briefly, images were separated into their channels, manually thresholded, and percent area of blue (nuclei) and green (cytosol) per image quantified (it was not possible to differentiate between cells using this method). Nuclear density (based upon Hoechst staining), density of GFP and relative density of cytosolic GFP provided measures of cytotoxicity.

In a further three experiments, 50B11 cells overexpressing GFP- $\alpha$ -synuclein + HCN1 or cells overexpressing GFP- $\alpha$ -synuclein + control plasmid were then treated with rotenone or DMSO for 48hrs (see Figure 8). Cells were then fixed with 4%PFA-sucrose, stained with Hoechst and imaged using epifluorescence (Zeiss Observer Z1, x20 objective with GFP and DAPI filters, 285 x 214 $\mu\text{m}$  image size, 15-30 images per quadrant, two technical replicates for each condition within each experiment).

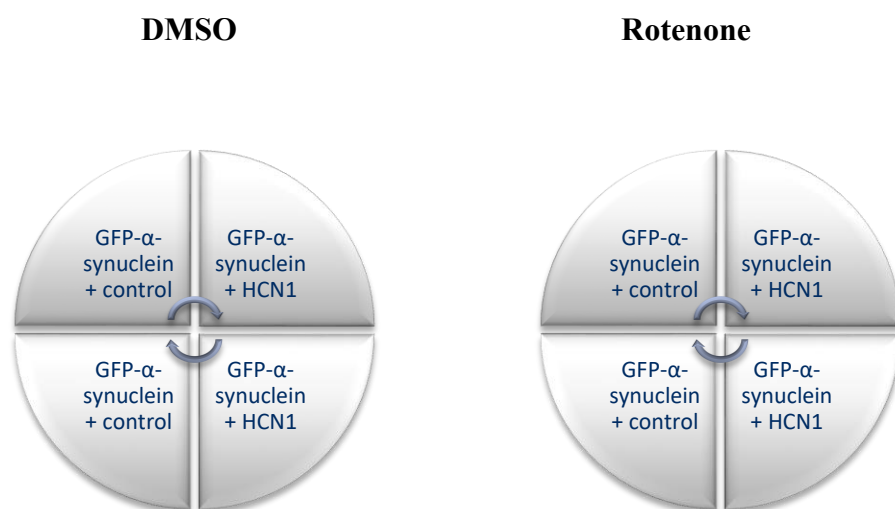


**Figure (8).** General experimental design for cytotoxicity analyses

These experiments examined whether HCN1 exacerbated effects of rotenone and/or  $\alpha$ -synuclein. Images were quantified for cytotoxicity by measuring area occupied by nuclei and area occupied by cytosol of transfected cells using CellProfiler. Briefly, cells expressing GFP (due to GFP- $\alpha$ -synuclein, all quadrants were transfected with GFP- $\alpha$ -synuclein) were identified by the software, based upon size and fluorescence intensity (see Figure 9A), then nuclei, based upon size and intensity, were identified (see Figure 9B), then nuclei within transfected cells were identified (see Figure 9C). As it was not possible to differentiate between cells, we measured total area occupied per image. This analysis was deliberately very conservative as the analysis was not channel-based as with confocal images, but rather based upon sizes and pixel intensities.

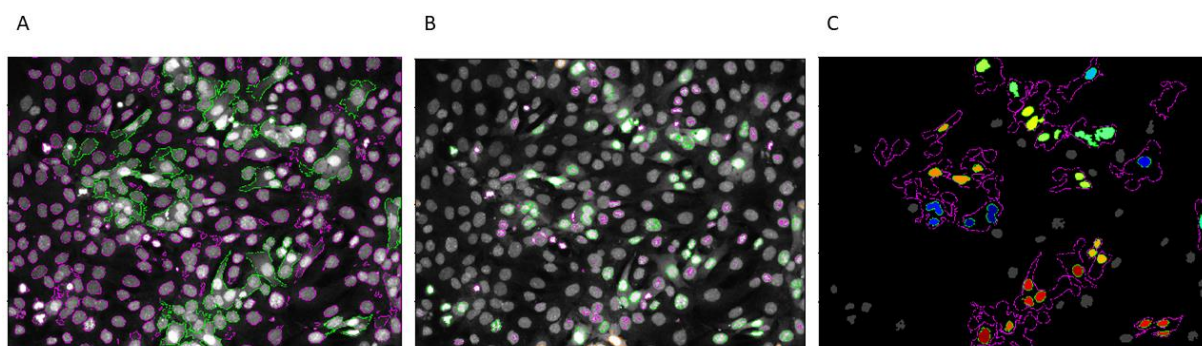


**Figure (9). CellProfiler analysis.** CellProfiler-based analysis of cytosol of transfected cells (A, green outlines), bright nuclei (B green outlines) and nuclei within transfected cells (C see coloured inserts within purple outlines). This analysis was deliberately very conservative as the imaging was not channel-based as with confocal images, but rather based upon sizes and pixel intensities.

### 3.1.8. Statistical Analysis

All experiments were performed at least in triplicate, with the researcher completely blinded for all image analyses. One-way or two-way ANOVAs were used for evaluation of statistical significance followed by post-hoc testing. For TMRM per-cell analyses, we used a Kruskal-Wallis 1-way ANOVA followed by Dunn's post-hoc tests because the software could not analyze these large datasets with more-appropriate two-way ANOVAs. All datasets were analyzed for parametric distribution. The criterion for significance was set to  $p < 0.05$ . Data visualization and analysis was conducted using GraphPad<sup>®</sup> Prism software (V9.3.1, CA, USA).

## 3.2 RESULTS

### 3.2.1 Effect of Overexpression of $\alpha$ -Synuclein on Parkinsonian 50B11 cells

$\alpha$ -Syn was overexpressed in 50B11 cells that were then treated with 100nM rotenone or DMSO (vehicle control) for 48hrs. This rotenone treatment protocol was previously established in our laboratory.

Confocal microscopic images of cells are shown in Figure (10) and quantification in Figure 11. Figure (11A) shows that exposure of 50B11 cells to rotenone led to a decrease in nuclear density in general (all nuclei quantified, not just nuclei of transfected cells, effect of treatment  $F(1, 103) = 55.8$ ,  $p < 0.0001$ ). When examining GFP signal, no change in percent area was observed between DMSO and rotenone, either in cells expressing control GFP plasmid or cells expressing  $\alpha$ -Synuclein (B; effect of treatment  $F(1, 103) = 0.08$ , ns). We note that the control GFP plasmid did not show the same efficiency of transfection as the  $\alpha$ -Synuclein GFP plasmid, as demonstrated by the reduced percent area occupied per image (B, effect of transfection  $F(1, 130) = 278.5$ ,  $p < 0.0001$ ). When normalising the GFP signal to total nuclei, we observed that  $\alpha$ -Synuclein may have protected cells from rotenone toxicity (C) as the relative area of transfected cells was increased in the  $\alpha$ -Synuclein + rotenone condition compared with  $\alpha$ -Synuclein + DMSO (C, treatment x transfection interaction,  $F(1, 233) = 7.2$ ,  $p < 0.01$ ). No such protection was observed in cells expressing control GFP. These data are interesting but not unexpected:  $\alpha$ -Synuclein has previously been shown to be protective in the context of the toxin maneb for example (Conde et al., 2023).

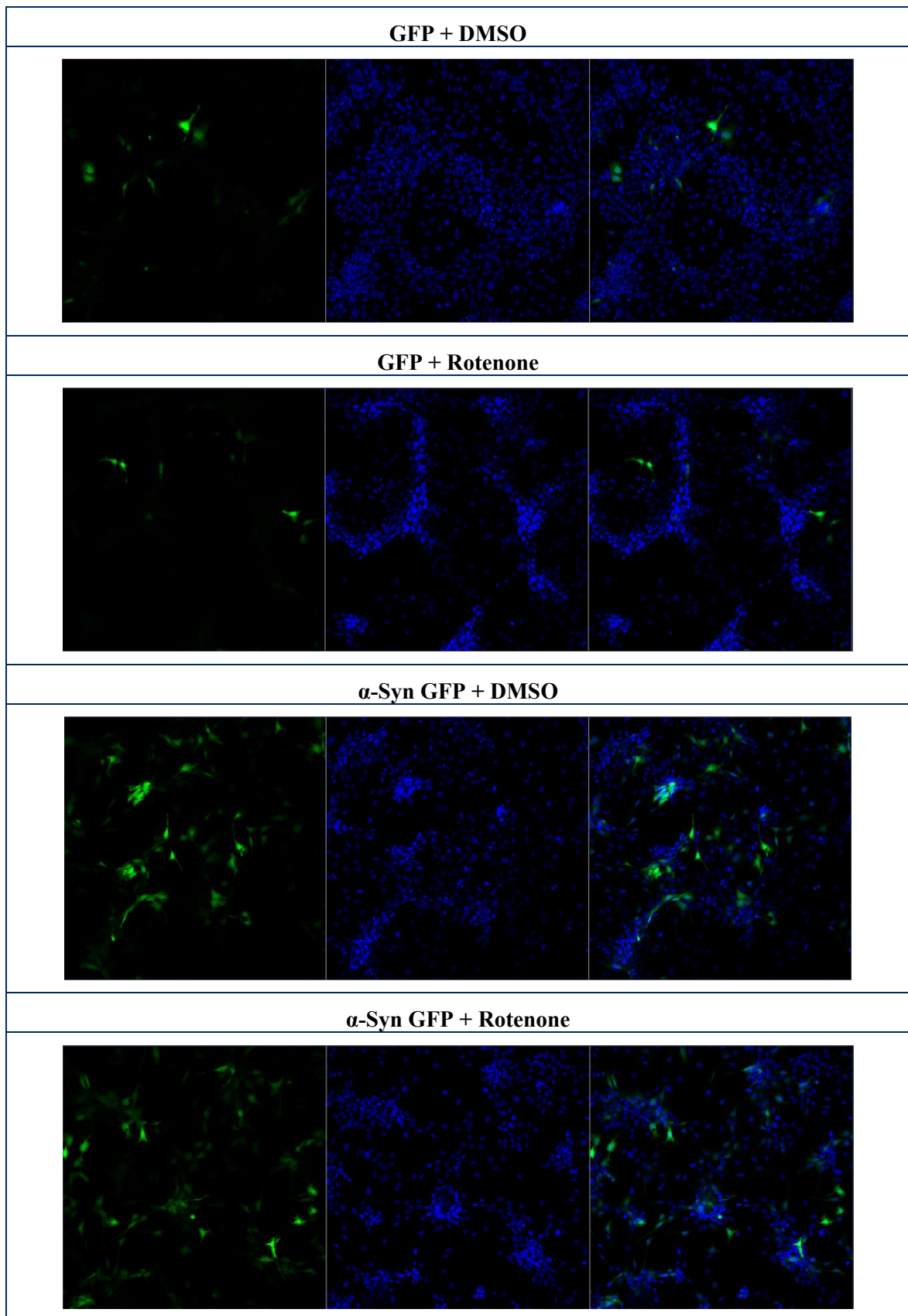


**Figure (10). Representative confocal microscopic images of 50B11 cells transfected with  $\alpha$ -Synuclein GFP or GFP control plasmid and then treated with DMSO or Rotenone. Merged images in right-most column show both fluorescent signals. The left-most column shows green fluorescence (either GFP control plasmid or  $\alpha$ -Synuclein GFP). The middle column shows nuclei stained with Hoechst.**



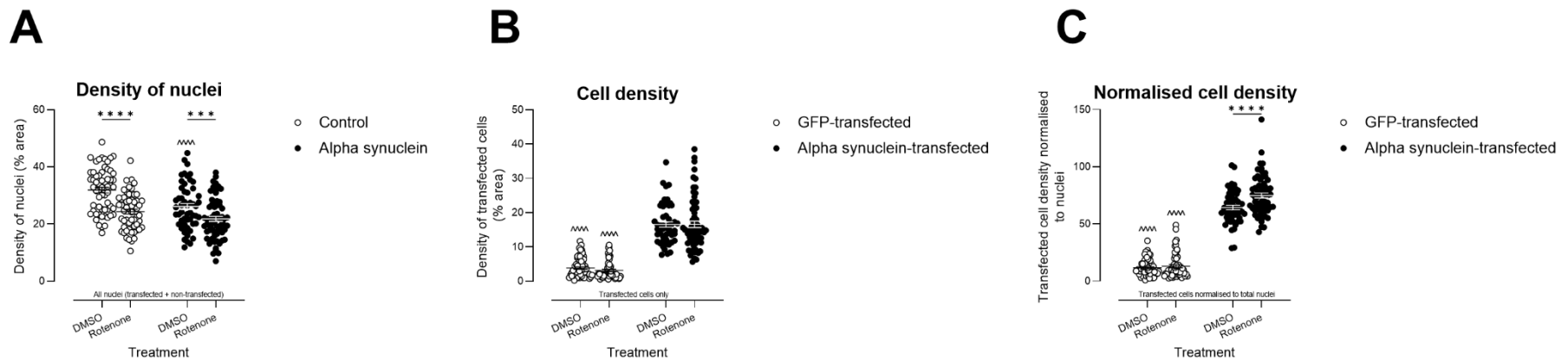


**Figure (11). Analysis of percent area covered by all nuclei (transfected + non-transfected), transfected cells and transfected cells normalised to total nuclei.** (A) Percent area covered by all nuclei.(B) Percent area covered by cells expressing GFP (GFP control plasmid or and  $\alpha$ -Syn).(C) Density of transfected cells normalized to nuclear percent area. Each data point on the graph represents an individual image. Horizontal bars show mean  $\pm$  SEM. Data were compared using two way ANOVA followed by post-hoc multiple comparisons. Asterisks indicate significant differences within groups(DMSO versus rotenone), whereas arrowheads indicate significant differences between groups ( $\alpha$ -Syn GFP + DMSO versus GFP + DMSO), \*\*\*\* $p < 0.0001$  for DMSO versus rotenone, within transfection groups. ^^^^  $p < 0.0001$  comparing between transfections, same treatment.

### 3.2.2 Effect of Overexpression of HCN1 on Parkinsonian 50B11 cells

As previously mentioned, the main aim of our study is to investigate the effect of overexpression of HCN1 in parkinsonian 50B11 cells because this channel is overexpressed in skin samples from PD patients (Planken et al., 2017) and hyperactivity of HCN1 channels are associated with PN (Resta et al., 2018).

As shown in Figure 12, HCN1 exacerbated the toxic effect of rotenone in 50B11 cells overexpressing  $\alpha$ -Syn, whether examining total area occupied by nuclei in transfected cells (A; treatment x transfection interaction,  $F(1, 300) = 8.8, p < 0.01$ ) or total area occupied by cytoplasm in transfected cells (B;  $F(1, 302) = 5.1, p < 0.05$ ). Here, we did not see a protective effect of  $\alpha$ -Syn when cells were exposed to rotenone (no HCN1, see white symbols). However, we note that data in Figure 12 are not normalised to total nuclear content (the protective effect was only noted in cells normalised to total nuclear count, see Figure 11). We aim to complete these additional analyses in the future. Thus, our data suggests that overexpression of HCN1 is toxic to sensory parkinsonian neurons.

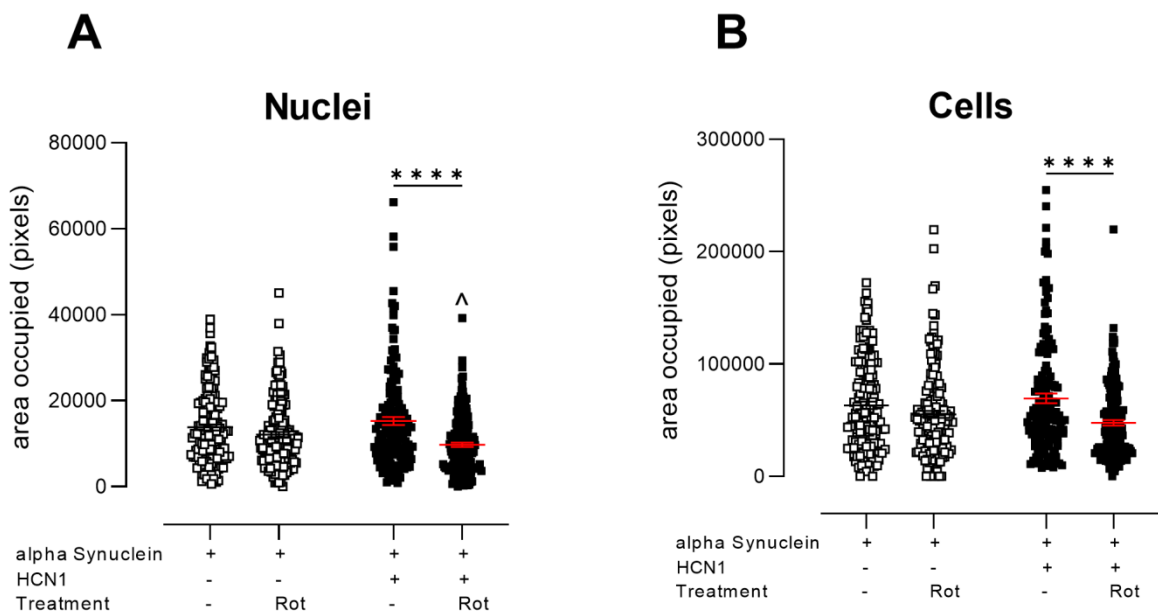


**Figure (12). Analysis of area occupied by nuclei (A) or cytoplasm (B) of parkinsonian 50B11.** 50B11 cells were transfected with  $\alpha$ -Syn GFP and control plasmid or HCN1 plasmid. Cells were then treated with DMSO or 100nM rotenone for 48hrs. A) Area occupied by Hoechst-labelled nuclei B) Area occupied by GFP-labelled cells. Each data point on the graph represents an individual image. Horizontal bars show mean  $\pm$  SEM. Data were compared using two way ANOVA, followed by post-hoc multiple comparison tests. Asterisks indicate significant differences within transfected groups (e.g. HCN1 + DMSO versus HCN1 + Rotenone). Arrowheads indicate significant differences within treated groups (e.g. control plasmid + DMSO versus HCN1 + DMSO)., \*\*\*\* $p < 0.0001$  ^ $p < 0.05$   $\alpha$ -Syn GFP + HCN1 + Rotenone versus  $\alpha$ -Syn GFP + rotenone.

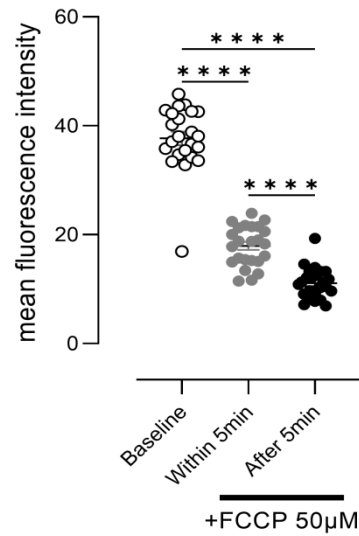
### **3.2.3 Effect of Overexpression of HCN1 on MMP**

#### **3.2.3.1. Demonstration of validity of method using FCCP, a mitochondrial uncoupler**

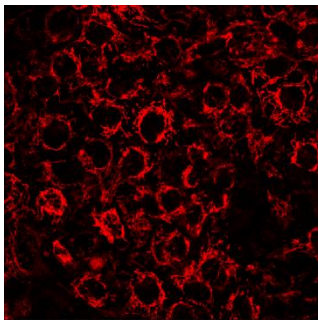
In mitochondria, complexes I through IV of the electron transport chain normally enable a build-up of protons in the mitochondrial inter-membrane space, which are then used to create ATP by Complex V. FCCP (carbonyl cyanide p-trifluoro methoxyphenylhydrazone) acts as a protonophore, enabling protons to flux through the inner cristae of the mitochondria and thereby preventing their use by Complex V to create ATP (Demine et al., 2019). FCCP causes mitochondria to transition from a well-coupled to an uncoupled state of respiration, which can be measured based upon the loss of mitochondrial sequestration of Tetramethylrhodamine methyl ester (TMRM). Here, FCCP was used as a positive control to demonstrate the efficacy of this outcome measurement (TMRM fluorescence).

TMRM fluorescence intensity was quantified at baseline and then at 2-5 min and 5-10 min after applying 50 $\mu$ M FCCP. A maximal effect of FCCP on TMRM signal was observed between 5-10min after application, where 50B11 cells expressed the lowest TMRM mean fluorescence intensity (Figure 13,  $F(1.7, 59.6) = 54.4, p < 0.0001$ ). These results demonstrate the validity of the TMRM method to detect changes in MMP in 50B11 cells.

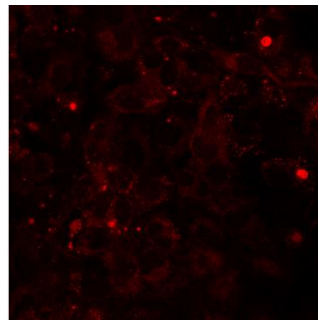
A



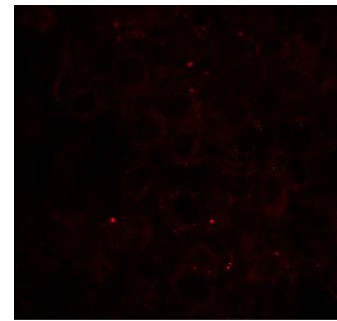
B



(i) Baseline (zero time)



(ii) 0- 5 min after FCCP



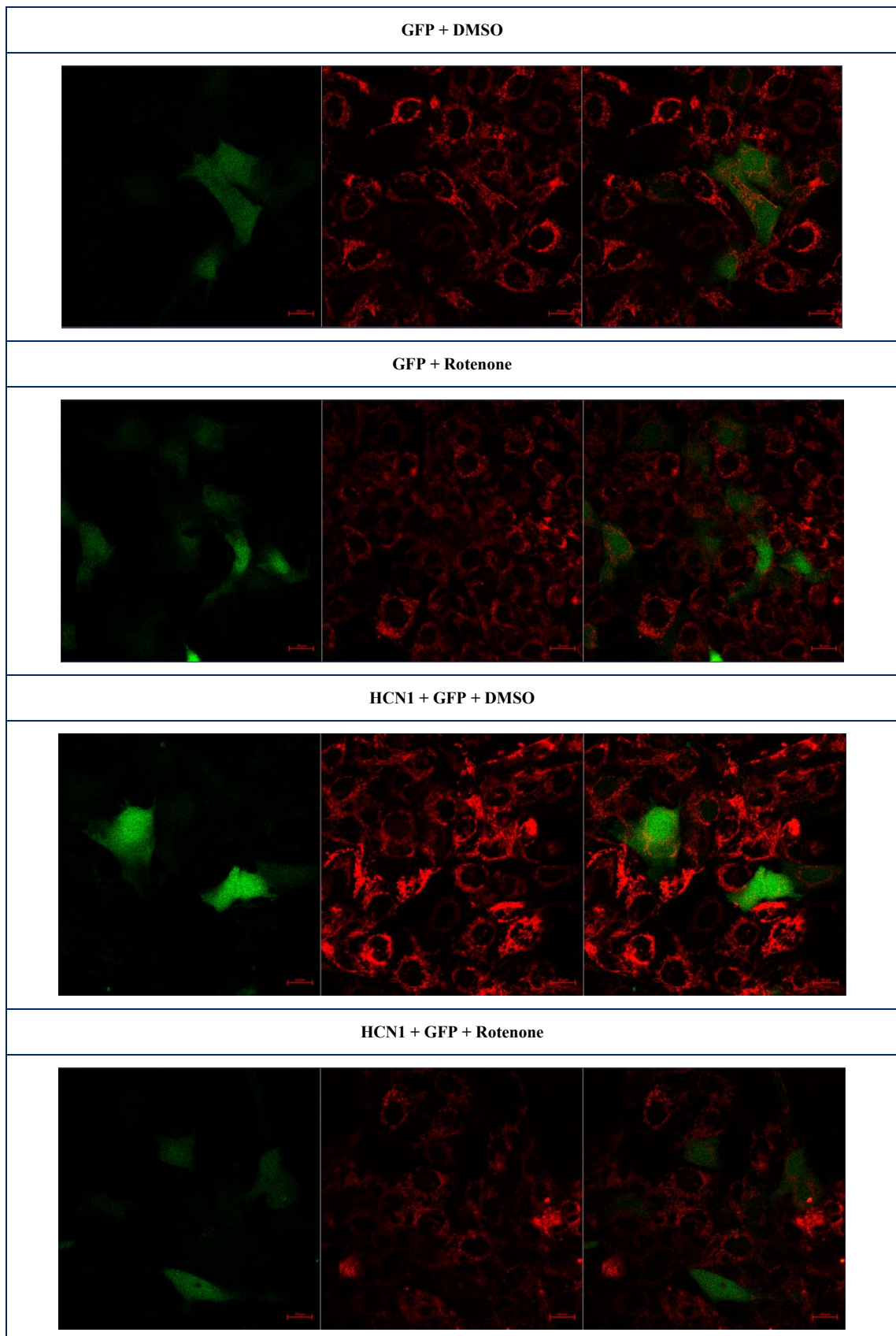
(iii) 5-10 min after FCCP

**Figure (13). Detection of loss of mitochondrial membrane potential: Positive-control experiment .** (A) Graphical representation of “TMRM mean fluorescence intensity” following application of FCCP. (B) Confocal microscopic images of 50B11 cells showing normal sequestration of TMRM in mitochondria at time zero. A progressive loss of TMRM fluorescence following treatment with FCCP, an uncoupler of mitochondrial oxidative phosphorylation, is observed. Each data point represents an image. Horizontal bars show mean  $\pm$  SE. Data were compared using a one-way ANOVA followed by post hoc tests. Asterisks indicate significant differences between time points \*\*\*\* $p < 0.0001$ . B) Photomicrographs demonstrating baseline TMRM fluorescence (left) and after 5mins of FCCP or 5-10mins after FCCP.

### **3.2.3.2. Effect of overexpression of HCN1 on MMP in parkinsonian 50B11 cells**

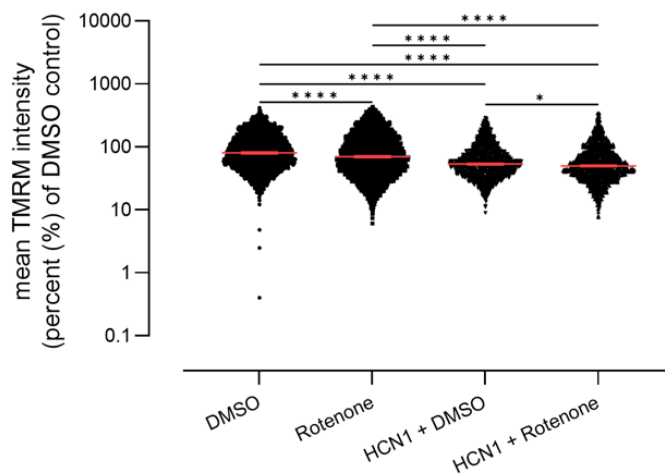
In these experiments, the effect of overexpression of HCN1 on MMP in parkinsonian 50B11 cells was examined. Parkinsonian 50B11 cells were generated by exposing them to rotenone.

Figure 14 shows representative confocal images of 50B11 cells overexpressing HCN1, using GFP as fluorescent biomarker of transfection. Cells were then treated with Rotenone or DMSO for 48hrs and then imaged live. HCN1-transfected cells appear as green fluorescent cells because they are co-transfected with a GFP-expressing plasmid. Mitochondria are represented in red (TMRM fluorescence). Untransfected cells appear as red (TMRM) with no associated green fluorescence.



**Figure (14).** Representative Confocal microscopic images of 50B11 cells expressing a control GFP plasmid or HCN1 + GFP and treated with DMSO or Rotenone. Green signal shows GFP/HCN1 co-transfected cells, while the TMRM mitochondrial stain appears as red signal in all cells. Merged images are shown on the right.

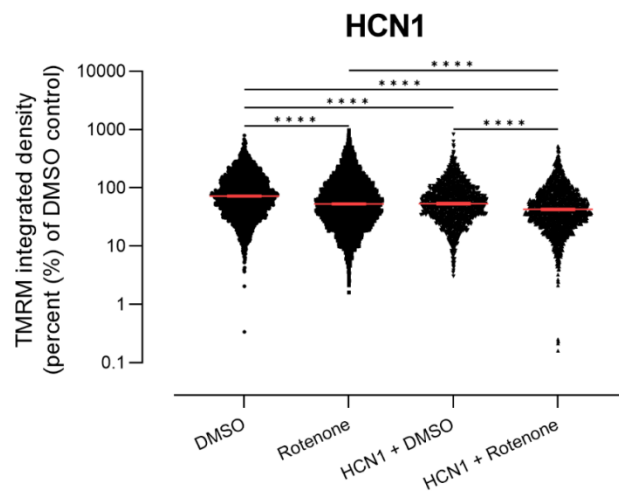
Results presented in Figure (15) show that rotenone treatment lead to a significant decrease in mean TMRM fluorescence in untransfected cells (cells that showed TMRM fluorescence only). Although the decrease was highly significant, it was slight, as mean TMRM intensity decreased by only 5%. This aligns with the expected sub-toxic effects of the rotenone concentration employed in our experiments. Overexpression of HCN1 alone lead to a large (34%) and significant decrease in mean TMRM fluorescence compared to untransfected cells. This shows a more pronounced effect of HCN1 on mitochondrial membrane potential than rotenone alone. Finally, 50B11 cells overexpressing HCN1 and treated with rotenone showed a small exacerbation of the effect of HCN1 alone, reducing TMRM fluorescence by 35.5% (Kruskal Wallis ANOVA:H (4, n = 14753) = 905.8,  $p < 0.0001$ ). To conclude, both rotenone and HCN1 caused mitochondrial depolarization, but overexpression of HCN1 showed a much stronger effect compared to rotenone, and a small additive effect was observed when cells overexpressing HCN1 were treated with rotenone.



**Figure (15). Mean TMRM fluorescence intensity, expressed relative to DMSO-treated untransfected cells.** 50B11 cells overexpressing HCN1 were then treated with DMSO or 100nM rotenone. Each data point on the graph represents an individual cell. Horizontal bars show median  $\pm$  95% confidence intervals. Data were compared using Kruskal-Wallis ANOVA, where median varied significantly at 95% confidence interval. This was followed by post-hoc multiple comparison tests. Asterisks indicate significant differences between groups. \* $p < 0.05$ , \*\*\*\* $p < 0.0001$ .

Given that a reduction in mean TMRM fluorescence intensity could reflect a loss in membrane potential or a loss in mitochondria, we also examined integrated intensity of TMRM staining. Integrated intensity of staining takes the area of staining into account (Figure 16); thus, a large area of moderate staining will have a greater integrated intensity than a small area of moderate staining. This outcome measure will provide an indirect measure of mitochondrial load. Results were in accordance with those presented in Figure 16, although a greater reduction in TMRM staining (41% reduced compared to DMSO-treated untransfected cells; Kruskal Wallis ANOVA  $H(4, n = 14753) = 599.4, p < 0.0001$ ) was observed following treatment with Rotenone in HCN1-expressing cells. These data suggest that mitochondrial load was affected in this condition. To investigate this in further detail, we examined overall cell sizes.

(A)



(B)

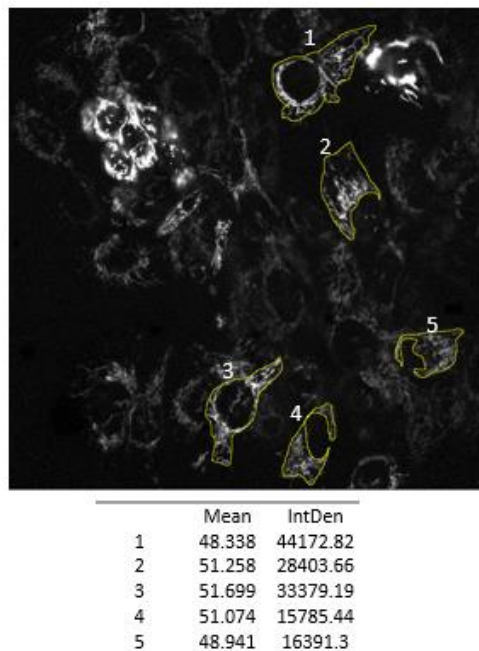


**Figure (16). Integrated density of TMRM fluorescence, expressed relative to DMSO-treated untransfected cells.** 50B11cells overexpressing HCN1 were then treated with DMSO or 100nM rotenone. (A) graphical representation of data. (B) Representative image showing differences in mean values versus integrated density of cells. Each data point on the graph represents an individual cell. Horizontal bars show median  $\pm$  95% confidence intervals. Data were compared using Kruskal-Wallis ANOVA. This was followed by post-hoc multiple comparison tests. Asterisks indicate significant differences between groups. \*\*\*\* $p < 0.0001$ .

As a further control, we examined the effect of expression of a control plasmid expressing GFP on TMRM fluorescence intensity. As shown in Figure 17, no effect on TMRM fluorescence (mean intensity: H (4, n = 1679) = 637.7,  $p < 0.0001$ ; integrated density: H (4, n = 1679) = 414.7,  $p < 0.0001$ ) was observed following overexpression of this plasmid. However, rotenone alone did have a greater effect in this experiment. This may be attributed to biological variability resulting from the small number of experiments involved in this analysis (n=1).

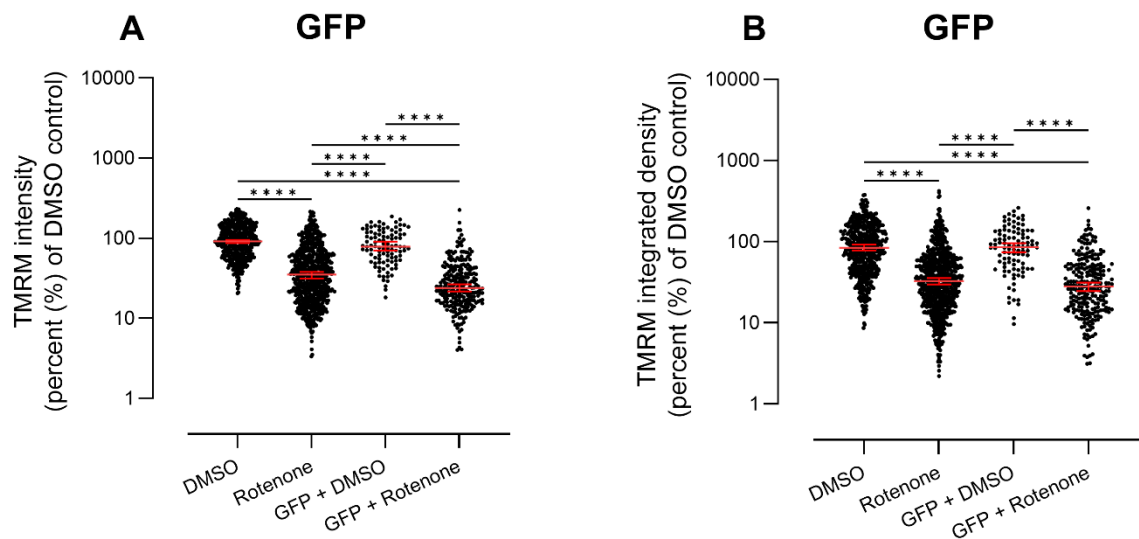


**Figure (17). Control experiment in 50B11 cells overexpressing GFP (control plasmid), followed by treatment with DMSO or 100nM rotenone. (A) Mean TMRM fluorescence intensity. (B) Integrated Density of TMRM fluorescence. Each data point on the graph represents an individual cell. Horizontal bars show median  $\pm$  95% confidence intervals. Data were compared using Kruskal-Wallis ANOVA. This was followed by post-hoc multiple comparison tests. Asterisks indicate significant differences between groups. \*\*\*\* $p < 0.0001$ .**

A reduction in mitochondrial area could also be due to reduced or altered cell size; thus, it was necessary to examine the effect of overexpression of HCN1 on the size of 50B11 cells (see Figure18). Results presented in Figure18A confirm that overexpression of HCN1 exacerbated the effect of rotenone on 50B11 cells, as shown by a significant decrease in the size of the cells. Control cells not expressing HCN1 GFP were not possible to measure and so the effect of HCN1 overexpression alone was not possible to examine. Rotenone

alone had no effect on cell size, as shown in Figure18B, where cells expressing control plasmid (expressing GFP only) were exposed to rotenone or DMSO.

Thus, although further studies are required to formally quantify mitochondrial load, e.g., using immunostaining or Western blotting, the reduction in TMRM staining suggests that mitochondrial load is reduced as both TMRM mean fluorescence intensity and mean integrated density are reduced. However, given that cell size is also reduced, it may also be important to examine mitochondrial density within individual cells.

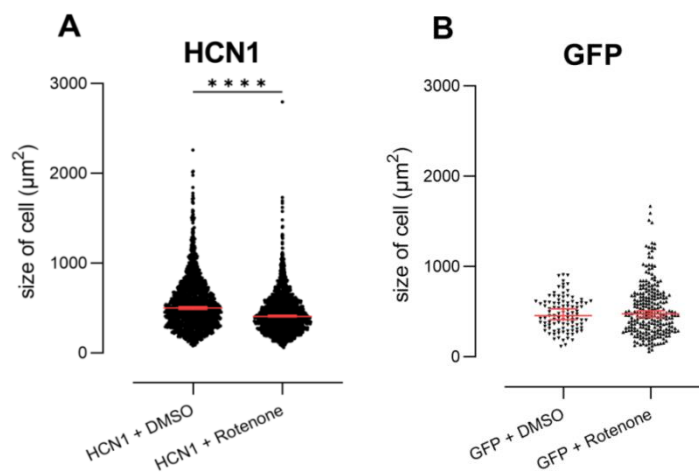


**Figure (18).** Effect of overexpression of HCN1 and rotenone on size of 50B11 cells. (A) Cells transfected with HCN1 or (B) control plasmid were treated with DMSO or rotenone. Each data point on the graph represents an individual cell. Horizontal bars show median  $\pm$  95% confidence intervals. Data were compared using Mann-Whitney U test. Asterisks indicate significant differences between groups, \*\*\*\* $p < 0.0001$

Having established that HCN1 overexpression 1) reduces mitochondrial membrane potential and 2) reduces cell size, we then went on to examine whether cell morphology was also affected using the CellProfiler outcomes of solidity and form factor, as shown in Figure19. The significant increase in solidity and in form factor observed in HCN1-expressing rotenone-treated cells implies that such cells tend to be rather spherical compared to those treated with DMSO, which have more protrusions. Figure (19C), shows

representative images of spherical cells and cells with protrusions. The normal morphology of 50B11 cells is to have protrusions.

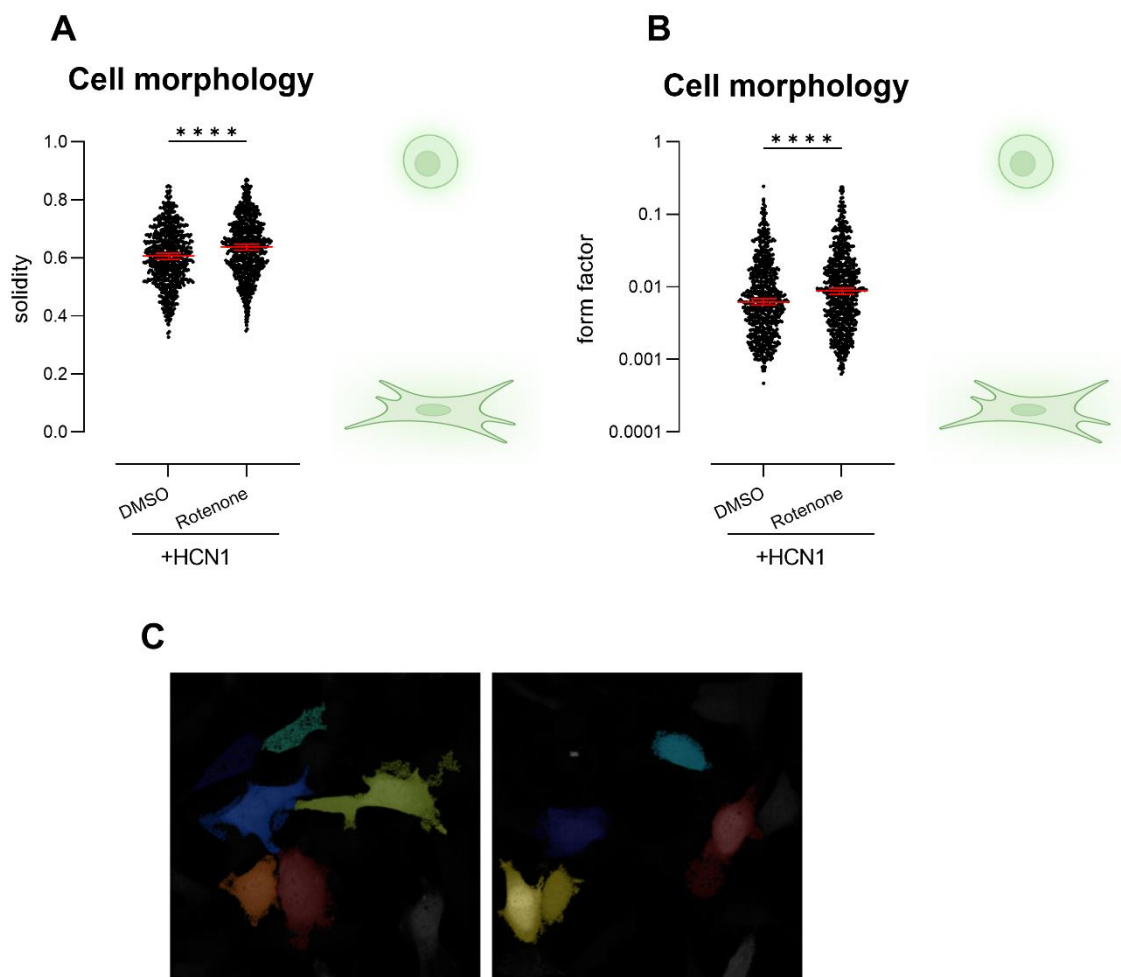


**Figure (19). Effect of overexpression of HCN1 and treatment with rotenone on morphology of 50B11 cells.** (A) Comparing solidity of cells treated with rotenone versus DMSO. (B) Comparing the form factor of cells treated with rotenone versus DMSO (C) Representative segmented images for HCN1 + DMSO (left) and HCN1 + Rotenone (right), following CellProfiler processing. Note the more rounded appearance of the HCN1 + rotenone-treated cells. Solidity data were compared using two tailed T-test ( $t= 5.75$ ,  $df= 1468$ ) at  $p<0.05$ . Form Factor data were compared using Mann-Whitney U test (two tailed). Horizontal bars show median  $\pm$  95% confidence interval. Asterisks indicate significant differences between groups. \*\*\*\* $p<0.0001$ .

### 3.2.4 Effect of Overexpression of SCN2B on 50B11 cells

This is a preliminary experiment that was carried out to evaluate overexpression of SCN2B on mitochondrial function in parkinsonian 50B11 cells (see Figure 20). SCN2B has also been reported as upregulated in PD patients' skin (Planken et al., 2017). In this experiment, as with our HCN1 experiments, rotenone caused a small (7%) but significant reduction in TMRM intensity in untransfected cells. SCN2B alone caused a greater reduction (31%) in mitochondrial membrane potential and exacerbated the effect of rotenone (34% reduction; Kruskal Wallis Anova:  $H(4, n = 3814) = 150.0, p < 0.0001$ ). Further work, currently in progress, will complete this series.

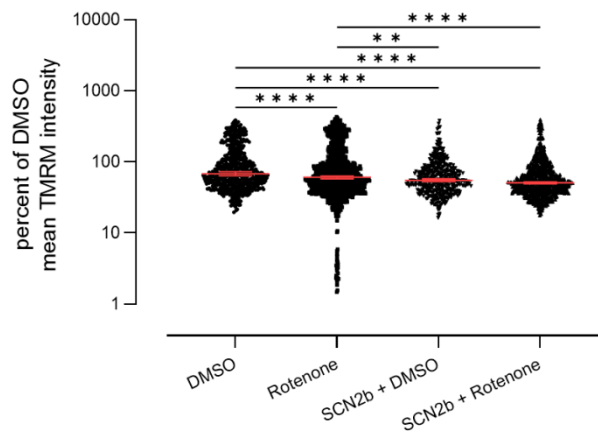


**Figure (20). Mean TMRM fluorescence intensity in 50B11 cells.** Cells overexpressing SCN2B were treated with DMSO or 100nM rotenone. TMRM fluorescence intensity was also examined in neighbouring untransfected cells. Each data point on the graph represents an individual cell. Horizontal bars show median  $\pm$  95% confidence intervals. Data were compared using Kruskal-Wallis ANOVA, followed by post-hoc multiple comparison tests. Asterisks indicate significant differences between groups, \*\* $p < 0.01$ , \*\*\*\* $p < 0.0001$

### **3.3 DISCUSSION**

#### **3.3.1. Effect of Overexpression of $\alpha$ -Synuclein and HCN1 on Cytotoxicity in Parkinsonian 50B11 cells**

Alpha-Synuclein ( $\alpha$ -Syn) overexpression and intracellular aggregation is a characteristic feature of PD pathology (Braak et al., 2003; Del Tredici & Braak, 2016). Mutation and overexpression of  $\alpha$ -Syn in the human leads to PD; it is undoubtedly toxic. Recent work has suggested that during the formation of Lewy bodies,  $\alpha$ -Syn is modified, and mitochondria, and lysosomal compartments are recruited, leading to gradual cytotoxicity (Mahul-Mellier et al., 2020). We have not yet quantified mitochondria or lysosomes in our  $\alpha$ -Syn-expressing cells; however, it forms part of our current work.

Interestingly, when we combined  $\alpha$ -Syn with rotenone, we found a protective effect, with increased density of  $\alpha$ -Syn-positive cells. This could be attributed  $\alpha$ -Syn-induced increased mitosis (Rodríguez-Losada et al., 2020). Or,  $\alpha$ -Syn could induce anti-oxidant gene transcription to induce a protective effect, as has been reported for the fungicide maneb (Conde et al., 2023). When the cells were further challenged by adding HCN1 overexpression, we did observe a combined cytotoxic effect of  $\alpha$ -Syn + HCN1 + Rotenone. Thus, our data suggests that the increased expression of HCN1, as has been reported in PD patient skin (Planken et al., 2017), can exacerbate toxicity of known risk factors for PD in sensory neurons.

#### **3.3.2. Effect of HCN1 on Mitochondria in Parkinsonian 50B11 cells**

Mitochondrial dysfunction has been reported in many neurodegenerative disorders, however; it is not always evident whether such dysfunction is a cause or a pathophysiological symptom of the underlying disease (Connolly et al., 2018). Certainly, mitochondrial dysfunction is strongly involved in the etiology of PD, more so than Alzheimer's disease for example, (Praschberger et al., 2023), as suggested by the strong increase in risk for PD following chronic exposure to complex I inhibitors, such as rotenone (Innos & Hickey, 2021).

Our results revealed that in-vitro exposure of 50B11 cells to rotenone, while overexpressing HCN1, resulted in mitochondrial depolarization, and that overexpression of

HCN1 showed a stronger effect compared to rotenone. In addition, HCN1 overexpression was observed to exacerbate the effect of rotenone. Some studies have highlighted a role for HCN1 channels in mitochondria; however, their function is largely unknown. It may be that they permit  $K^+$  entry into the mitochondrial matrix; however, in doing so, they enable water and anion to follow thereby resulting in mitochondrial swelling (Benzoni et al., 2021; Szabo & Szewczyk, 2023). Moreover; a mild mitochondrial uncoupling effect of HCN3 channels has been reported in the nephron (León-Aparicio et al., 2019). This would further justify the significantly low levels of mean TMRM fluorescence intensity achieved when HCN1 was overexpressed in 50B11 cells.

The reduction in mean TMRM fluorescence could be due to a general reduction in mitochondrial membrane potential. However, integrated intensity of TMRM staining suggested that loss of mitochondrial volume was a factor. But, a change in cell size could also play a role. Alteration of cell morphology, upon overexpression of HCN1 in cells treated with rotenone, from its normal, fibroblast-like morphology form to a more spherical form could be attributed to several possible causes. Mitosis and cell proliferation might be considered. Lancaster et al. suggested that cells would morphologically change from flat to spherical under mitotic conditions (Lancaster et al., 2013). However, cells also retract processes as an indicator of toxicity (Bisbal et al., 2018). In current work, we are examining these questions.

## **SUMMARY**

PD symptoms developing along the prodromal phase has been of great interest especially that the available therapeutic strategies of PD focus basically on motor symptoms, appearing at late stages of the disease. PD patients with PN have been increasingly reported. PD patients' kin biopsies examined by our research collaborators in Tartu University Hospital revealed an upregulation in HCN1 excitatory ion channels and SCN2B regulatory ion channel. This encouraged our research team to investigate the effect of overexpression of these channels, with a major focus on HCN1. Overexpression of HCN1 was examined in the context of genetic and environmental PD risk factors represented in rotenone and alphasynuclein, respectively, and their interaction. Immortalized 50B11 cells were used as our experimental cell line, for studying the effect of overexpression of HCN1 excitatory ion channel on mitochondrial membrane potential and cytotoxicity in parkinsonian sensory neurons. Cytotoxicity data suggested that increased expression of HCN1 can exacerbate toxicity of known risk factors for PD in sensory neurons. Similarly, TMRM analysis results revealed that HCN1 overexpression was observed to exacerbate the effect of rotenone, through an observed significant reduction in mean TMRM fluorescence that was suggested to be attributed to loss of mitochondria rather than general mitochondrial depolarization. Additionally, HCN1 was found to affect cell morphology normal, fibroblast-like morphology form to a more spherical form, suggesting possible toxicity or proliferative effect of overexpression of HCN1 in parkinsonian 50B11 cells. In general, further immunoassays and other investigations are still ongoing in order to have a clearer image of our research question.

## REFERENCES

- Alsaloum M., Labau J.I.R., Sosniak D., Zhao P., Almomani R., Gerrits M., Hoeijmakers J.G.J., Lauria G., Faber C.G., Waxman S.G., Dib-Hajj S. A novel gain-of-function sodium channel  $\beta$ 2 subunit mutation in idiopathic small fiber neuropathy. *Journal of Neurophysiology*, 2021, 126 (3): 827-839
- Alves G., Forsaa E. B., Pedersen K. F., Dreetz Gjerstad M., Larsen J. P. Epidemiology of Parkinson's disease. *J. Neurol.*, 2008, 255: 18–32.
- Ascherio A., Schwarzschild M.A. The epidemiology of Parkinson's disease: risk factors and prevention, *Lancet Neurol.*, 2016, 15: 1257–1272
- Balestrino R., Schapira A.H.V. Review: Parkinson disease *European Journal of Neurology* 2020, 27: 27–42. doi:10.1111/ene.14108
- Barbuti A., Baruscotti M., DiFrancesco D. The pacemaker current: from basics to the clinics. *J. Cardiovasc. Electrophysiol.*, 2007a, 18, 342–347. doi: 10.1111/j.1540-8167.2006.00736.x
- Baruscotti M., Bottelli G., Milanesi R., DiFrancesco J.C., DiFrancesco D. HCN-related channelopathies. *Pflugers Arch.*, 2010, 460: 405–415. doi: 10.1007/s00424-010-0810-8
- Beaulieu M.L., Müller M., Bohnen N.I. Peripheral neuropathy is associated with more frequent falls in Parkinson's disease. *Parkinsonism RelatDisord.*, 2018, 54: 46–50
- Beitz J.M. Skin and wound issues in patients with Parkinson's disease: an overview of common disorders. *Ostomy Wound Manage*, 2013, 59 (6): 26–36
- Bellou V., Belbasis L., Tzoulaki I., Evangelou E., Ioannidis J.P. Environmental risk factors and Parkinson's disease: an umbrella review of meta-analyses. *Parkinsonism Relat Disord.*, 2016, 23:1–9. <https://doi.org/10.1016/j.parkreldis.2015.12.008>
- Bennett D.L., Clark A.J., Huang J., Waxman S.G., Dib-Hajj S.D. The role of voltage-gated sodium channels in pain signaling. *Physiol Rev*, 2019, 99: 1079–1151. doi:10.1152/physrev.00052.2017
- Betarbet R., Canet-Aviles R.M., Sherer T.B., Mastroberardino P.G., McLendon C., Kim J.H., Lund S., Na H.M., Taylor G., Bence N.F., Kopito R., Seo B.B., Yagi T., Yagi A., Klinefelter G., Cookson M.R., Greenamyre J.T.. Intersecting pathways to neurodegeneration in Parkinson's disease: effects of the pesticide rotenone on DJ-1, alpha-synuclein, and the ubiquitin-proteasome system. *Neurobiol Dis*, 2006, 22: 404-420

- Biel M., Wahl-Schott C., Michalakis S., Zong X. Hyperpolarization-activated cation channels: from genes to function. *Physiol. Rev.*, 2009, 89, 847–885. doi: 10.1152/physrev.00029.2008
- Bloem B.R., Okun M.S., Klein C. Parkinson's disease. *The Lancet*, 2021, 397 (10291): 2284-2303. [https://doi.org/10.1016/S0140-6736\(21\)00218-X](https://doi.org/10.1016/S0140-6736(21)00218-X)
- Braak H., Del T.K., Rub U. de Vos R.A., Jansen Steur E.N., Braak E. Staging of brain pathology related to sporadic Parkinson's disease. *Neurobiol. Aging*, 2003, 24:197–211
- Bulling M.T., Wing L.M., Burns R.J. Controlled release levodopa/carbidopa (Sinemet CR4) in Parkinson's disease—an open evaluation of efficacy and safety. *Aust. NZ J. Med.*, 1991, 21 (4) : 397–400.
- Cappellano G., Carecchio M., Fleetwood T., Magistrelli L., Cantello R., Dianzani U., Comi C. Immunity and inflammation in neurodegenerative diseases. *Am J Neurodegener Dis.*, 2013, 2(2): 89-107
- Catterall W.A., Linares M.J., Gamal El-Din T.M. Structure and pharmacology of voltage-gated sodium and calcium channels. *Annu Rev PharmacolToxicol*, 2020, 60: 133–154. doi:10.1146/annurevpharmtox-010818-021757
- Ceravolo R., Cossu G., Poggio M.B., Santoro L., Barone P., Zibetti M., Frosini D., Nicoletti V., Manganelli F., Iodice R., Picillo M., Merola A., Lopiano L., Paribello A., Manca D., Melis M., Marchese R., Borelli P., Mereu A., Contu P., Abbruzzese G., Bonuccelli U. Neuropathy and levodopa in Parkinson's disease: evidence from a multicenter study. *Mov Disord.*, 2013, 28 (10): 1391-1397. doi: 10.1002/mds.25585
- Choi J.H., Kim J.M., Yang H.K., Lee H.J., Shin C.M., Jeong S.J., Won-Soek K., Ji Won H., In-Young Y., Yoo-Sung S., Yun Jung B. Clinical Perspectives of Parkinson's Disease for Ophthalmologists, Otorhinolaryngologists, Cardiologists, Dentists, Gastroenterologists, Urologists, Psychiatrists, and Psychiatrists. *J Korean Med Sci.*, 2020, 35 (28): e230. <https://doi.org/10.3346/jkms.2020.35.e230>
- Chu Y., Morfini G.A., Langhamer L.B., He Y., Brady S.T., Kordower J.H. Alterations in axonal transport motor proteins in sporadic and experimental Parkinson's disease. *Brain*, 2012, 135: 2058e73
- Comi C., Magistrelli L., Oggioni G.D., Carecchio M., Fleetwood T., Cantello R., Mancini F., Antonini A. Peripheral nervous system involvement in Parkinson's disease: evidence and controversies. *Parkinsonism Relat Disord.*, 2014, 20 (12): 1329-1334. doi: 10.1016/j.parkreldis.2014.10.010

- Conde M.A., Alza N.P., Funk M.I., Maniscalchi A., Benzi Juncos O.N., Berge I., Uranga R.M., Salvador G.A.  $\alpha$ -Synuclein Attenuates Maneb Neurotoxicity through the Modulation of Redox-Sensitive Transcription Factors. *Oxid Med Cell Longev.*, 2023, 2023:5803323. doi: 10.1155/2023/5803323
- Connolly N.M.C., Theurey P., Adam-Vizi V., Bazan N.G., Bernardi P., Bolaños J.P., Culmsee C., Dawson V.L., Deshmukh M., Duchen M.R., Düssmann H., Fiskum G., Galindo M.F., Hardingham G.E., Hardwick J.M., Jekabsons M.B., Jonas E.A., Jordán J., Lipton S.A., Manfredi G., Mattson M.P., McLaughlin B.A., Methner A., Murphy A.N., Murphy M.P., Nicholls D.G., Polster B.M., Pozzan T., Rizzuto R., Satrústegui J., Slack R.S., Swanson R.A., Swerdlow R.H., Will Y., Ying Z., Joselin A., Gioran A., Pinho C.M., Watters O., Salvucci M., Llorente-Folch I., Park D.S., Bano D., Ankarcróna M., Pizzo P., Prehn J.H.M. Review article: Guidelines on experimental methods to assess mitochondrial dysfunction in cellular models of neurodegenerative diseases. *Cell Death & Differentiation*, 2017, 25(3): 542- 572, <https://doi.org/10.1038/s41418-017-0020-4>
- Cornelis B. Mike A.N, Andrew B.S. The genetic architecture of Parkinson's disease. *The Lancet Neurology*, 2019, S147444221930287X. doi:10.1016/S1474-4422(19)30287-X
- Dabby R., Djaldetti R., Shahmurov M., Treves T.A., Gabai B., Melamed E., Sadeh M., Avinoach I. Skin biopsy for assessment of autonomic denervation in Parkinson's disease. *J Neural Transm (Vienna)*, 2006, 113 (9): 1169-1176. doi: 10.1007/s00702-005-0431-0
- Del Rey N.L., Quiroga-Varela A., Garbayo E., Carballo-Carbajal I., Fernández-Santiago R., Monje M.H.G., Trigo-Damas I., Blanco-Prieto M.J., Blesa J. Advances in Parkinson's Disease: 200 Years Later. *Front Neuroanat.*, 2018, 12: 113. doi: 10.3389/fnana.2018.00113
- Del Tredici K.; Braak H. Review: Sporadic Parkinson's disease: development and distribution of  $\alpha$ -synuclein pathology. *Neuropathology and Applied Neurobiology*, 2016, 42 (1): 33–50. doi:10.1111/nan.12298
- DiFrancesco J.C., DiFrancesco D. Dysfunctional HCN ion channels in neurological diseases. *Front. Cell. Neurosci.*, 2015, 9: 71. doi: 10.3389/fncel.2015.00071
- Dini L., Del Lungo M., Resta F., Melchiorre M., Spinelli V., Di Cesare Mannelli L., Ghelardini C., Laurino A., Sartiani L., Coppini R., Mannaioni G., Cerbai E., Romanelli M.N. Selective Blockade of HCN1/HCN2 Channels as a Potential Pharmacological Strategy Against Pain. *Front. Pharmacol.*, 2018, 9:1252. doi: 10.3389/fphar.2018.01252

- Donadio V., Incensi A., Leta V., Giannoccaro M.P., Scaglione C., Martinelli P., Capellari S., Avoni P., Baruzzi A., Liguori R. Skin nerve  $\alpha$ -synuclein deposits: a biomarker for idiopathic Parkinson disease, *Neurology*, 2014, 82 (15): 1362–1369
- Doppler K., Ebert S., Uçeyler N., Trenkwalder C., Ebentheuer J., Volkmann J., Sommer C. Cutaneous neuropathy in Parkinson's disease: a window into brain pathology. *Acta Neuropathol.*, 2014, 128 (1): 99–109. doi: 10.1007/s00401-014-1284-0
- Dorsey E.R., Constantinescu R., Thompson J.P., Biglan K.M., Holloway R.G., Kieburtz K., Marshall F.J., Ravina B.M., Schifitto G., Siderowf A., Tanner C.M. Projected number of people with Parkinson disease in the most populous nations, 2005 through 2030. *Neurology*, 2007, 68(5): 384-386. doi: 10.1212/01.wnl.0000247740.47667.03
- Dorsey E.R., Sherer T., Okun M.S., Bloem B.R. The emerging evidence of the Parkinson pandemic. *J Parkinsons Dis*, 2018, 8: S3-S8
- Dunning C.J., Reyes J.F., Steiner J.A., Brundin P. Can Parkinson's disease pathology be propagated from one neuron to another? *Prog. Neurobiol.*, 2012, 97: 205–219
- Eijkenboom I., Sopacua M., Hoeijmakers J.G.J., de Greef B.T.A., Lindsey P., Almomani R., Marchi M., Vanoevelen J., Smeets H.J.M., Waxman S.G., Lauria G., Merkies I.S.J., Faber C.G., Gerrits M.M. Yield of peripheral sodium channels gene screening in pure small fibre neuropathy. *J Neurol Neurosurg Psychiatry*, 2019, 90: 342–352. doi:10.1136/jnnp-2018-319042
- Emery E.C., Young G.T., Berrocoso E.M., Chen L., McNaughton P.A. HCN2 ion channels play a central role in inflammatory and neuropathic pain. *Science*, 2011, 333: 1462–1466. doi: 10.1126/science.1206243
- Emmanouilidou E., Stefanis L., Vekrellis K. Cell-produced alpha-synuclein oligomers are targeted to, and impair, the 26S proteasome. *Neurobiol. Aging*, 2010, 31: 953–968
- Farrer M.J., Williams L.N., Algom A.A., Kachergus J., Hulihan M.M., Ross O.A., Rajput A., Papapetropoulos S., Mash D.C., Dickson D.W. Glucosidase-beta variations and Lewy body disorders. *Parkinsonism Relat. Disord.*, 2009, 15: 414–416 doi: 10.1016/Zj.parkreldis.2008.08.004
- Fayyad M., Salim S., Majbour N., Erskine D., Stoops E., Mollenhauer B., El-Agnaf O.M.A. Review: Parkinson's disease biomarkers based on  $\alpha$ -synuclein. *International Society for Neurochemistry, J. Neurochem.*, 2019, 150: 626-636
- Friedrich T., van Heek P., Leif H., Ohnishi T., Forche E., Kunze B., Janen R., Trowitzsch-Kienast W., Höfle G., Reichenbach H., et al. Two binding sites of inhibitors in NADH: ubiquinone oxidoreductase (complex I). Relationship of one site with the ubiquinone-

- binding site of bacterial glucose:ubiquinone oxidoreductase. *Eur J Biochem.* 1994 Jan 15;219(1-2):691-8. doi: 10.1111/j.1432-1033.1994.tb19985.x
- Mahul-Mellier A.-L., Burtscher J., Maharjan N., Weerens L., Croisier M., Kuttler F., ... Lashuel, H.A. The process of Lewy body formation, rather than simply  $\alpha$ -synuclein fibrillization, is one of the major drivers of neurodegeneration. *Proceedings of the National Academy of Sciences*, 2020, 117 (9): 4971–4982. doi:10.1073/pnas.1913904117
- Giannoccaro M.P., Donadio V., Incensi A., Pizza F., Cason E., Di Stasi V., Martinelli P., Scaglione C., Capellari S., Treglia G., Liguori R. Skin biopsy and I-123 MIBG scintigraphy findings in idiopathic Parkinson's disease and parkinsonism: a comparative study, *Mov. Disord.*, 2015, 30 (7): 986–989
- Gnaiger E., Aasander Frostner E., Abdul Karim N., Abdel-Rahman E.A., Abumrad N.A., Acuna-Castroviejo D., Adiele R.C., Ahn B., Alencar M.B., Ali S.S., et al. Mitochondrial respiratory states and rates. *MitoFit Preprint Arch.*, 2019, doi: 10.26124/mitofit:190001.v5
- Halliday G.M., Holton J.L., Revesz T., Dickson D.W. Neuropathology underlying clinical variability in patients with synucleinopathies. *Acta Neuropathol.*, 2011, 122, 187–204
- Hammarlund C.S., Westergren A., Åström I., Edberg A.K., Hagell P. The impact of living with Parkinson's disease: balancing within a web of needs and demands. *Parkinsons Dis.* 2018, 2018: 4598651
- Hanewincke R., Drenthen J., van Oijen M., Hofman A., van Doorn P.A., Ikram M.A. Prevalence of polyneuropathy in the general middle-aged and elderly population, *Neurology*, 2016, 87 (18): 1892–1898
- Hatcher J.M., Pennell K.D., Miller G.W. Parkinson's disease and pesticides: a toxicological perspective. *Trends Pharmacol Sci*, 2008, 29: 322-329
- Heikkila R.E., Nicklas W.J., Vyas I., Duvoisin R.C. Dopaminergic toxicity of rotenone and the 1-methyl-4-phenylpyridinium ion after their stereotaxic administration to rats: implication for the mechanism of 1-methyl-4-phenyl-1,2,3,6-tetrahydropyridine toxicity. *Neurosci Lett*, 1985, 62: 389-394
- Heinz S., Freyberger A., Lawrenz B., Schladt L., Schmuck G., Ellinger-Ziegelbauer H. Mechanistic Investigations of the Mitochondrial Complex I Inhibitor Rotenone in the Context of Pharmacological and Safety Evaluation. *Sci Rep*, 2017, 7: 45465

- Hernandez Fustes O.J., Hernandez Fustes O.J. Sensory Neuropathy in Parkinson Disease: Electrodiagnostic Evaluation. *The Neurodiagnostic Journal*, 2020, 60: 177–184. doi: 10.1080/21646821.2020.1796414
- Hernandez D.G., Reed X., Singleton A.B. Genetics in Parkinson disease: Mendelian versus non-Mendelian inheritance. *J Neurochem.*, 2016,139: 59–74
- Innos J., Hickey M.A. Using Rotenone to Model Parkinson's Disease in Mice: A Review of the Role of Pharmacokinetics. *Chem Res Toxicol*, 2021, 34 (5):1223-1239. doi: 10.1021/acs.chemrestox.0c00522
- Ishii T.M., Takano M., Ohmori H. Determinants of activation kinetics in mammalian hyperpolarization-activated cation channels. *J. Physiol.*, 2001, 537: 93e100
- Jellinger K.A. Neuropathology of sporadic Parkinson's disease: evaluation and changes of concepts. *Mov. Disord*, 2012, 27: 8–30
- Kalia L.V., Lang A.E. Parkinson's disease. *The Lancet*, 2015, 386 (9996): 896-912. [https://doi.org/10.1016/S0140-6736\(14\)61393-3](https://doi.org/10.1016/S0140-6736(14)61393-3)
- Karpinar D.P., Balija M.B., Kugler S., Opazo F., Rezaei-Ghaleh N., Wender N., Kim H.Y., Taschenberger G., Falkenburger B.H., Heise H., Kumar A., Riedel D., Fichtner L., Voigt A., Braus G.H., Giller K., Becker S., Herzig A., Baldus M., Jackle H., Eimer S., Schulz J.B., Griesinger C., Zweckstetter M. Pre-fibrillar  $\alpha$ -synuclein variants with impaired  $\beta$ -structure increase neurotoxicity in Parkinson's disease models, *Embo J*, 2009, 28: 3256–3268
- Kass-Iliyya L., Javed S., Gosal D., Kobylecki C., Marshall A., Petropoulos I.N., Ponirakis G., Tavakoli M., Ferdousi M., Chaudhuri K.R., Jeziorska M., Malik R.A., Silverdale M.A. Small fiber neuropathy in Parkinson's disease: a clinical, pathological and corneal confocal microscopy study, *Parkinsonism Relat. Disord.*, 2015, 21 (12): 1454–1460
- Kaushik S., Cuervo A.M. Proteostasis and aging. *Nat. Med.*, 2015, 2: 1406–1415
- Kiebertz K., Wunderle K.B. Parkinson's disease: evidence for environmental risk factors. *Mov Disord*, 2013, 28: 8–13.
- Lancaster M.A., Renner M., Martin C.A., Wenzel D., Bicknell L.S., Hurler M.E., Homfray T., Penninger J.M., Jackson A.P., Knoblich J.A. Cerebral organoids model human brain development and microcephaly. *Nature*, 2013; 501(7467):373-9. doi: 10.1038/nature12517
- Langston J.W., Ballard P., Tetrud J.W., Irwin I. Chronic parkinsonism in humans due to a product of meperidine-analog synthesis. *Science*, 1983, 219: 979–880

- Magistrelli L., Contaldi E., Comi C. The Impact of SNCA Variations and Its Product Alpha-Synuclein on Non-Motor Features of Parkinson's Disease. *Life*, 2021, 11: 804
- Mancini F., Comi C., Oggioni G.D., et al. Prevalence and features of peripheral neuropathy in Parkinson's disease patients under different therapeutic regimens. *Parkinsonism Relat Disord.*, 2014, 20 (1): 27–31.
- Martinez-Vicente M., Talloczy Z., Kaushik S., Massey A.C., Mazzulli J., Mosharov E.V., Hodara R., Fredenburg R., Wu D.C., Follenzi A., Dauer W., Przedborski S., Ischiropoulos H., Lansbury P.T., Sulzer D., Cuervo A.M. Dopamine-modified alpha-synuclein blocks chaperone-mediated autophagy. *J Clin Invest.*, 2008, 118b(2): 777-788. doi: 10.1172/JCI32806
- McGinty R.N., McNamara B., Moore H. DADS neuropathy associated with anti-TNF $\alpha$  therapy, *BMJ Case Rep.*, 2015:bcr2015211781, <http://dx.doi.org/10.1136/bcr-2015-211781>
- Misra U.K., Kalita J., Nair P.P. Diagnostic approach to peripheral neuropathy. *Ann Indian Acad Neurol.*, 2008,11(2): 89–97
- Nalls M.A. et al. Large-scale meta-analysis of genomewide association data identifies six new risk loci for Parkinson's disease. *Nat. Genet.*, 2014, 46: 989–993. This paper is a large meta-analysis of GWAS that describes the genetic variants that alter the risk for Parkinson disease.
- Nalls M.A., Blauwendraat C., Vallerga C.L., et al. Expanding Parkinson's disease genetics: novel risk loci, genomic context, causal insights and heritable risk. *bioRxiv*, 2019, doi:10.1101/388165
- Nolano M., Provitera V., Estraneo A., Selim M.M., Caporaso G., Stancanelli A., Saltalamacchia A.M., Lanzillo B., Santoro L. Sensory deficit in Parkinson's disease: evidence of a cutaneous denervation. *Brain*, 2008, 131:1903–1911
- Nolano M., Provitera V., Lanzillo B., Santoro L. Neuropathy in idiopathic Parkinson disease: an iatrogenic problem? *Ann. Neurol.*, 2011, 69 (2): 427–428
- Novak P., Marya N.B., Whren K., Bhawan J. Dermal sheet preparations in the evaluation of dermal innervation in Parkinson's disease and multiple system atrophy, *J. Cutan. Pathol.*, 2009, 36 (3): 296–301
- Noyce A.J., Lees A.J., Schrag A.E. The prediagnostic phase of Parkinson's disease. *J Neurol Neurosurg Psychiatry*, 2016, 87: 871–878
- Pang S.Y-Y, Ho P.W-L., Liu H-F., Leung C-T., Li L., Chang E.E., Ramsden D.B., Ho S-L. The interplay of aging, genetics and environmental factors in the pathogenesis of

- Parkinson's disease. *Translational Neurodegeneration*, 2019, 8: 23. doi: 10.1186/s40035-019-0165-9
- Pérez-Villalba A., Sirerol-Piquer M.S., Belenguer G., Soriano-Cantón R., Muñoz-Manchado A.B., Villadiego J. Synaptic regulator  $\alpha$ -synuclein in dopaminergic fibers is essentially required for the maintenance of subependymal neural stem cells. *J Neurosci.*, 2018, 38:814–825
- Perry S.W., Norman J.P., Barbieri J., Brown E.B., Gelbard H.A. Review: Mitochondrial membrane potential probes and the proton gradient: a practical usage guide. *BioTechniques*, 2011, 50: 98-115. doi 10.2144/000113610
- Pertin M., Ji R.R., Berta T., Powell A.J., Karchewski L., Tate S.N., Isom L.L., Woolf C.J., Gilliard N., Spahn D.R., Decosterd I. Upregulation of the voltage-gated sodium channel beta2 subunit in neuropathic pain models: characterization of expression in injured and non-injured primary sensory neurons. *J Neurosci.*, 2005, 25(47): 10970-10980. doi: 10.1523/JNEUROSCI.3066-05.2005
- Planken A., Kurvits L., Reimann E., Kadastik-Eerme L., Kingo K., Kõks S., Taba P. Looking beyond the brain to improve the pathogenic understanding of Parkinson's disease: implications of whole transcriptome profiling of Patients' skin. *BMC Neurology*, 2017, 17: 6. doi: 10.1186/s12883-016-0784-z
- Poewe W., Seppi K., Tanner C.M., Halliday G.M., Brundin P., Volkmann J., Schrag A.E., Lang A.E. Parkinson disease. *Nat Rev Dis Primers*, 2017, 3: 17013. doi: 10.1038/nrdp.2017.13. PMID: 28332488
- Polymeropoulos M.H., Lavedan C., Leroy E., Ide S.E., Dehejia A., Dutra A., Pike B., Root H., Rubenstein J., Boyer R., Stenroos E.S., Chandrasekharappa S., Athanassiadou A., Papapetropoulos T., Johnson W.G., Lazzarini A.M., Duvoisin R.C., Di Iorio G., Golbe L.I., Nussbaum R.L. Mutation in the alpha-synuclein gene identified in families with Parkinson's disease. *Science*, 1997, 276 (5321): 2045-2047. doi: 10.1126/science.276.5321.2045
- Praschberger R., Kuenen S., Schoovaerts N., Kaempf N., Singh J., Janssens J., Swerts J., Nachman E., Calatayud C., Aerts S., Poovathingal S., Verstreken P. Neuronal identity defines  $\alpha$ -synuclein and tau toxicity. *Neuron*, 2023, 17; 111 (10): 1577-1590.e11. doi: 10.1016/j.neuron
- Reed X., Bandres-Ciga S., Blauwendraat C., Cookson M.R. The role of monogenic genes in idiopathic Parkinson's disease. *Neurobiol Dis.*, 2019, 124:230–239

- Resta F., Micheli L., Laurino A., Spinelli V., Mello T., Sartiani L., Mannelli L.D., Cerbai E., Ghelardini C., Romanelli M.N., Mannaioni G., Masi A. Selective HCN1 block as a strategy to control oxaliplatin-induced neuropathy. *Neuropharmacology*, 2018, 131: 403–413. doi: 10.1016/j.neuropharm.2018.01.014
- Rietdijk C.D., Perez-Pardo P., Garssen J., van Wezel R.J.A., Kraneveld A.D. Exploring Braak's Hypothesis of Parkinson's Disease. *Front. Neurol.*, 2017, 8: 37. doi: 10.3389/fneur.2017.00037
- Robinson R.B., Siegelbaum S.A. Hyperpolarization-activated cation currents: from molecules to physiological function. *Annu. Rev. Physiol.*, 2003, 65: 453–480. doi: 10.1146/annurev.physiol.65.092101.142734
- Rodríguez-Losada N., de la Rosa J., Larriva M., Wendelbo R., Aguirre J.A., Castresana J.S., Ballaz S.J. Overexpression of alpha-synuclein promotes both cell proliferation and cell toxicity in human SH-SY5Y neuroblastoma cells. *J Adv Res*, 2020, 22; 23: 37-45. doi: 10.1016/j.jare.2020.01.009
- Romagnolo A., Merola A., Artusi C.A., Rizzone M.G., Zibetti M., Lopiano L. Levodopa-induced neuropathy: A systematic review. *Mov Disord Clin Pract.*, 2019, 6 (2): 96–103
- Schrag A., Anastasiou Z., Ambler G., Noyce A., Walters K. Predicting diagnosis of Parkinson's disease: a risk algorithm based on primary care presentations. *Mov Disord*, 2019, 34: 480–486
- Schrag A., Bohlken J., Dammertz L., Teipel S., Hermann W., Akmatov M.K., Bätzing J., Holstiege J. Widening the Spectrum of Risk Factors, Comorbidities, and Prodromal Features of Parkinson Disease. *JAMA Neurol.*, 2023, 80 (2): 161-171. doi: 10.1001/jamaneurol.2022.3902
- Shahrizaila N., Mahamad U.A., Yap A.C., Choo Y.M., Marras C., Lim S.Y. Is chronic levodopa therapy associated with distal symmetric polyneuropathy in Parkinson's disease? *Parkinsonism Relat. Disord.*, 2013, 19 (3): 391–393
- Singleton A.B., Farrer M.J., Bonifati V. The genetics of Parkinson's disease: progress and therapeutic implications. *Mov. Disord.*, 2013, 28: 14–23. doi: 10.1002/mds.25249
- Singleton A., Hardy J. A generalizable hypothesis for the genetic architecture of disease: pleomorphic risk loci. *Hum. Mol. Genet.*, 2011, 20: R158–R162 10.1093/hmg/ddr358
- Singleton A., Hardy J. The evolution of genetics: Alzheimer's and Parkinson's diseases. *Neuron*, 2016, 90: 1154–1163

- Spillantini M.G., Crowther R.A., Jakes R., Hasegawa M., Goedert M. Alphasynuclein in filamentous inclusions of lewy bodies from parkinson's disease and dementia with lewy bodies. *Proc Natl Acad Sci USA*, 1998, 95: 6469–6473
- Stern M.B., Lang A. Poewe W. Toward a redefinition of Parkinson's disease. *Mov. Disord*, 2012, 27: 54–60
- Stirling D.R., Swain-Bowden M.J., Lucas A.M., Carpenter A.E., Cimini B.A., Goodman A. CellProfiler 4: improvements in speed, utility and usability. *BMC Bioinformatics*, 2021, 22 (1), 433. PMID: 34507520 PMCID: PMC8431850. ([www.cellprofiler.org](http://www.cellprofiler.org))
- Szabo I., Szewczyk A. Mitochondrial Ion Channels. *Annual Review of Biophysics*, 2023, 52:1, 229-254.
- Takamatsu Y., Fujita M., Ho G.J., Wada R., Sugama S., Takenouchi T., Waragai M., Masliah E., Hashimoto M. Motor and Nonmotor Symptoms of Parkinson's Disease: Antagonistic Pleiotropy Phenomena Derived from  $\alpha$ -Synuclein Evolvability? *Parkinsons Dis.*, 2018, 2018:5789424. doi: 10.1155/2018/5789424
- Tanik S.A., Schultheiss C.E., Volpicelli-Daley L.A., Brunden K.R., Lee V.M. Lewy body-like alphasynuclein aggregates resist degradation and impair macroautophagy. *J. Biol. Chem.*, 2013, 288: 15194–15210
- Tanner C.M., Kamel F., Ross G.W., Hoppin J.A., Goldman S.M., Korell M., Marras C., Bhudhikanok G.S., Kasten M., Chade A.R., Comyns K., Richards M.B., Meng C., Priestley B., Fernandez H.H., Cambi F., Umbach D.M., Blair A., Sandler D.P., Langston J.W. Rotenone, paraquat, and Parkinson's disease. *Environ Health Perspect*, 2011, 119(6): 866-872. doi: 10.1289/ehp.1002839
- Themistocleous A.C., Ramirez J.D., Serra J., Bennett D.L. The clinical approach to small fibre neuropathy and painful channelopathy, *Pract. Neurol.*, 2014, 14 (6): 368–379
- Thomas R., Kim M.H. Targeting the hypoxia inducible factor pathway with mitochondrial uncouplers. *Molecular and Cellular Biochemistry*, 2007, 296 (1-2): 35-44
- Van Den Eeden S.K., Tanner C.M., Bernstein A.L., Fross R.D., Leimpeter A., Bloch D.A., Nelson L.M. Incidence of Parkinson's disease: variation by age, gender, and race/ethnicity. *Am J Epidemiol.*, 2003, 157(11):1015-22. doi: 10.1093/aje/kwg068. PMID: 12777365
- Vega J.A., López-Muñiz A., Calavia M.G., García-Suárez O., Cobo J., Otero J., Arias-Carrión O., Pérez-Piñera P., Menéndez-González M. Clinical implication of Meissner's corpuscles. *CNS Neurol Disord Drug Targets.*, 2012, 11(7): 856-868

- Wang N., Gibbons C.H., Lafo J., Freeman R. Alpha-Synuclein in cutaneous autonomic nerves. *Neurology.*, 2013, 81 (18): 1604–1610
- Wang Z., Becker K., Donadio V., Siedlak S., Yuan J., Rezaee M., Incensi A., Kuzkina A., Orrú C.D., Tatsuoka C., Liguori R., Gunzler S.A., Caughey B., Jimenez-Capdeville M.E., Zhu X., Doppler K., Cui L., Chen S.G., Ma J., Zou W.Q. Skin  $\alpha$ -Synuclein Aggregation Seeding Activity as a Novel Biomarker for Parkinson Disease. *JAMA Neurol.*, 2020, 78 (1): 1–11. doi: 10.1001/jamaneurol.2020.3311
- Winner B., Jappelli R., Maji S.K., Desplats P.A., Boyer L., Aigner S., Hetzer C., Loher T., Vilar M., Campioni S., Tzitzilonis C., Soragni A., Jessberger S., Mira H., Consiglio A. Pham E., Masliah E., Gage F.H., Riek R. In vivo demonstration that alpha-synuclein oligomers are toxic. *Proc Natl Acad Sci USA*, 2011, 108 (10): 4194-41999. doi: 10.1073/pnas.1100976108
- Wolters E. Non-motor extranigral signs and symptoms in Parkinson’s disease. *Parkinsonism Relat Disord.*, 2009,15 Suppl 3:S6–12.
- Xilouri M., Brekk O.R., Stefanis L. Alphasynuclein and protein degradation systems: a reciprocal relationship. *Mol. Neurobiol.*, 2013, 47: 537–551
- Xilouri M., Vogiatzi T., Vekrellis K., Park D., Stefanis L. Abberant alpha-synuclein confers toxicity to neurons in part through inhibition of chaperone mediated autophagy. *PLoS ONE*, 2009, 4: e5515
- Xu X., Shang Y., Jiang J. Plant species forbidden in health food and their toxic constituents, toxicology and detoxification *Food Funct.*, 2016, 7(2):643-64. doi: 10.1039/c5fo00995b
- Zimmermann M. Pathobiology of neuropathic pain. *Eur J Pharmacol.*, 2001, 19; 429 (1-3): 23-37. doi: 10.1016/s0014-2999(01)01303-6
- Zis P., Grünewald R.A., Chaudhuri R.K., Hadjivassiliou M. Peripheral neuropathy in idiopathic Parkinson’s disease: A systematic review. *J Neurol Sci.*, 2017, 378: 204–209
- Zis P., Sarrigiannis P.G., Rao D.G., Hewamadduma C., Hadjivassiliou M. Chronic idiopathic axonal polyneuropathy: a systematic review, *J. Neurol.*, 2016, 263 (10): 1903–1910

## **NON-EXCLUSIVE LICENCE TO REPRODUCE THESIS AND MAKE THESIS PUBLIC**

**I, Iman Muhammad Higazy AbdelHamid Higazy EL-Talb**

1. Here with grant the University of Tartu a free permit (non-exclusive licence) to reproduce, for the purpose of preservation, including for adding to the DSpace digital archives until the expiry of the term of copyright,

### **Investigation of excitatory ion channels on parkinsonian sensory neurons**

supervised by **Associate Professor, Miriam Hickey, PhD, and Researcher, Maili Jakobson, PhD**

2. I grant the University of Tartu a permit to make the work specified in p. 1 available to the public via the web environment of the University of Tartu, including via the DSpace digital archives, under the Creative Commons licence CC BY NC ND 3.0, which allows, by giving appropriate credit to the author, to reproduce, distribute the work and communicate it to the public, and prohibits the creation of derivative works and any commercial use of the work until the expiry of the term of copyright.

3. I am aware of the fact that the author retains the rights specified in p. 1 and 2.

4. I certify that granting the non-exclusive licence does not infringe other persons' intellectual property rights or rights arising from the personal data protection legislation.

*Author's name Imane Higazy*



*25/06/2023*